Using Inelastic Spectra to Determine the Spin States of Multiferroic Materials

Randy Fishman, Oak Ridge National Laboratory

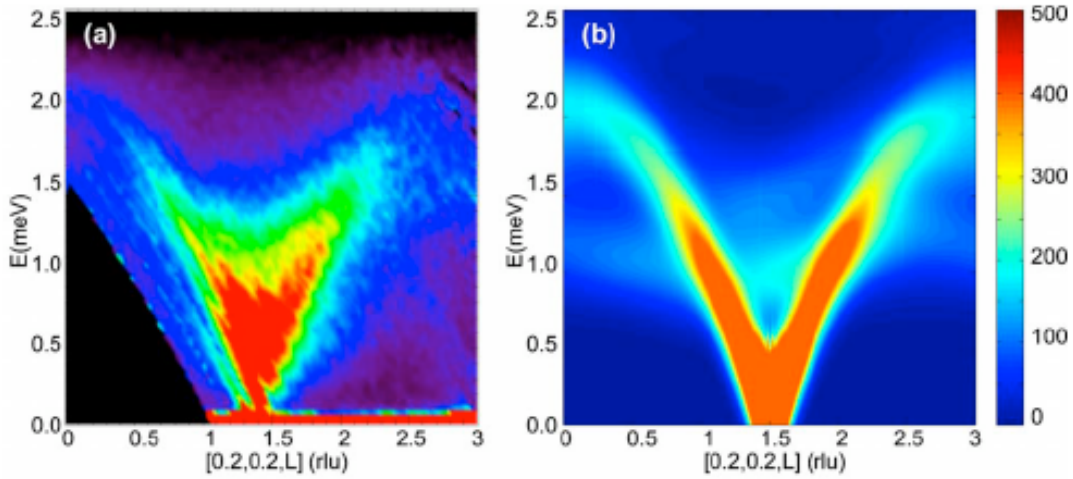

Supported by the Division of Materials Sciences and Engineering of the U.S. Department of Energy

University of Louisiana, Baton Rouge
February 12, 2015

OAK RIDGE NATIONAL LABORATORY
MANAGED BY UT-BATTELLE FOR THE DEPARTMENT OF ENERGY

Outline

1. **Elastic scattering and its limitations**
2. **The dynamical fingerprint of a spin state**
3. **Multiferroic materials**
4. **A Type II multiferroic: $CuFeO_2$**
5. **A Type I multiferroic: $BiFeO_3$**
6. **Numerical considerations**
7. **Conclusion**

1. Elastic scattering and its limitations

Many materials of current interest have complex spin states. For example, $CuFeO_2$ has a distorted spiral state

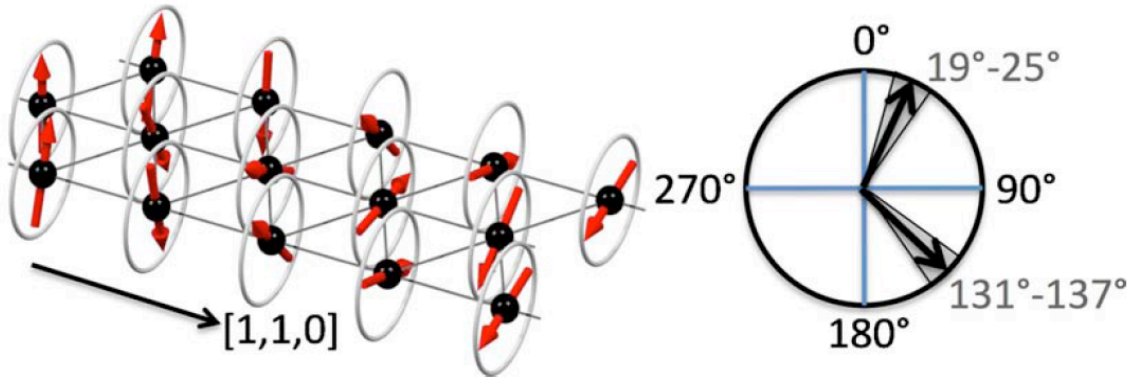

and $Ni_3V_2O_8$ has a magnetic unit cell containing 60 unique sites:

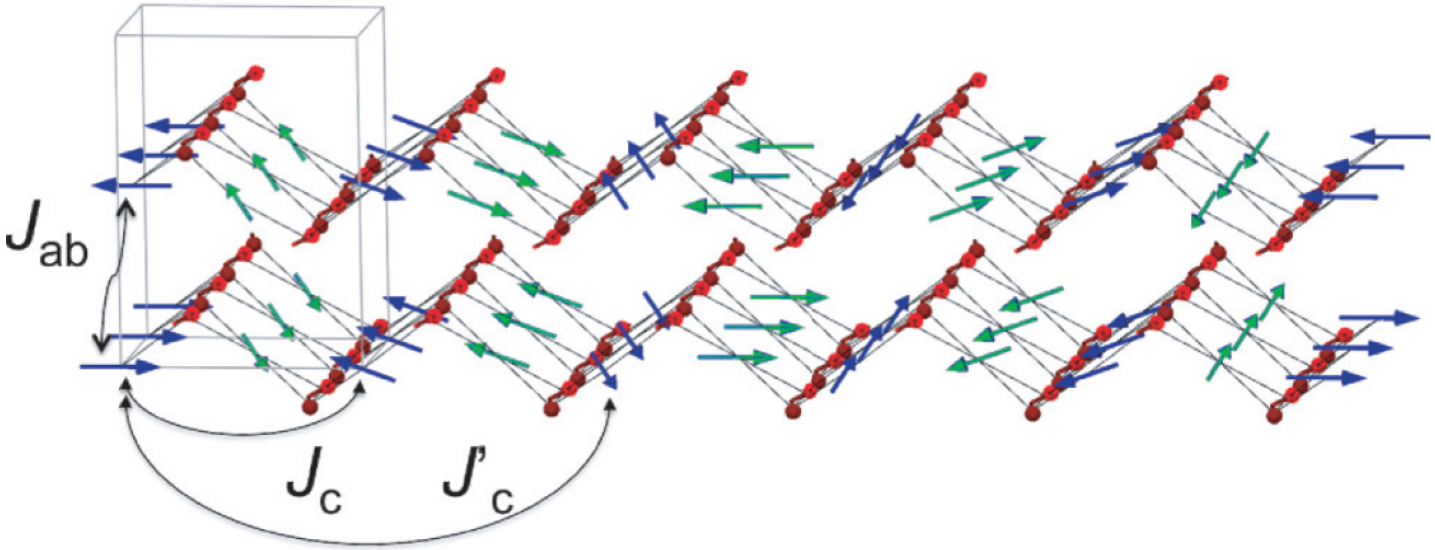

In principle, elastic ($\omega = 0$) neutron scattering can determine any spin state *if* you know all the elastic peaks *and* their intensities.

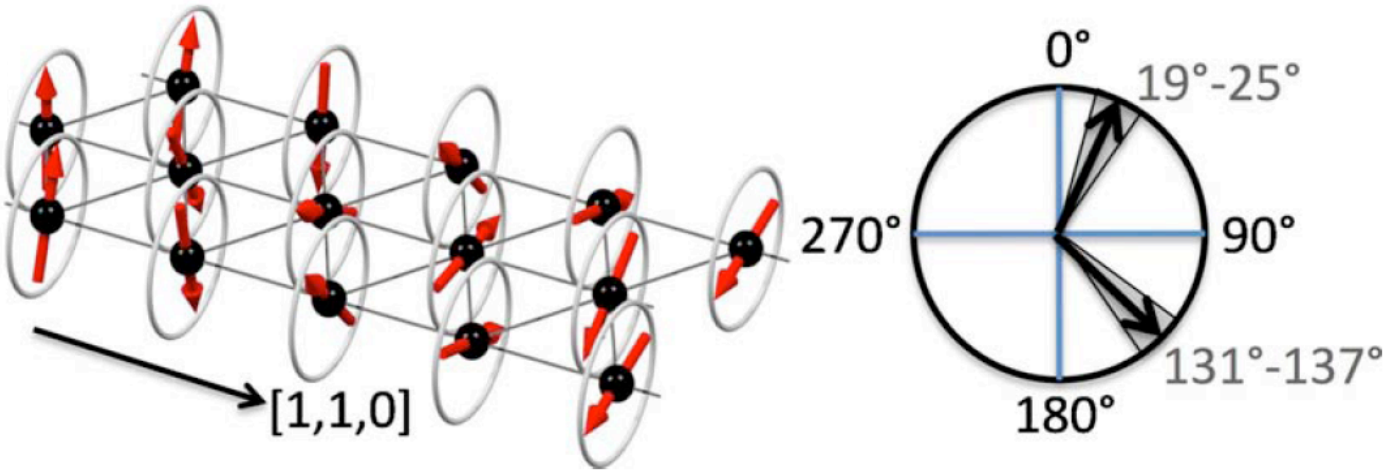

In practice, many peaks are too weak to observe and only a few are detected. For example, the elastic measurements on the right do not tell us enough to determine the spin state of $CuFeO_2$ above.

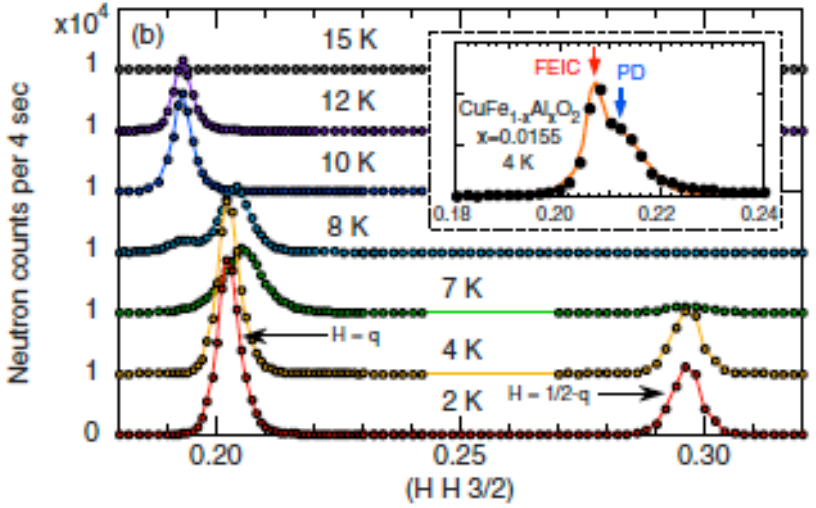

Even knowing all the peak wavevectors and intensities, elastic scattering alone cannot determine the magnetic interactions.

Consider a simple ferromagnet (FM) like Fe with all of the spins aligned.

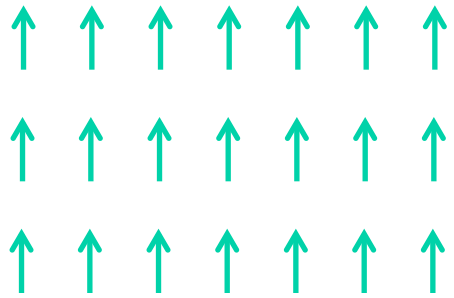

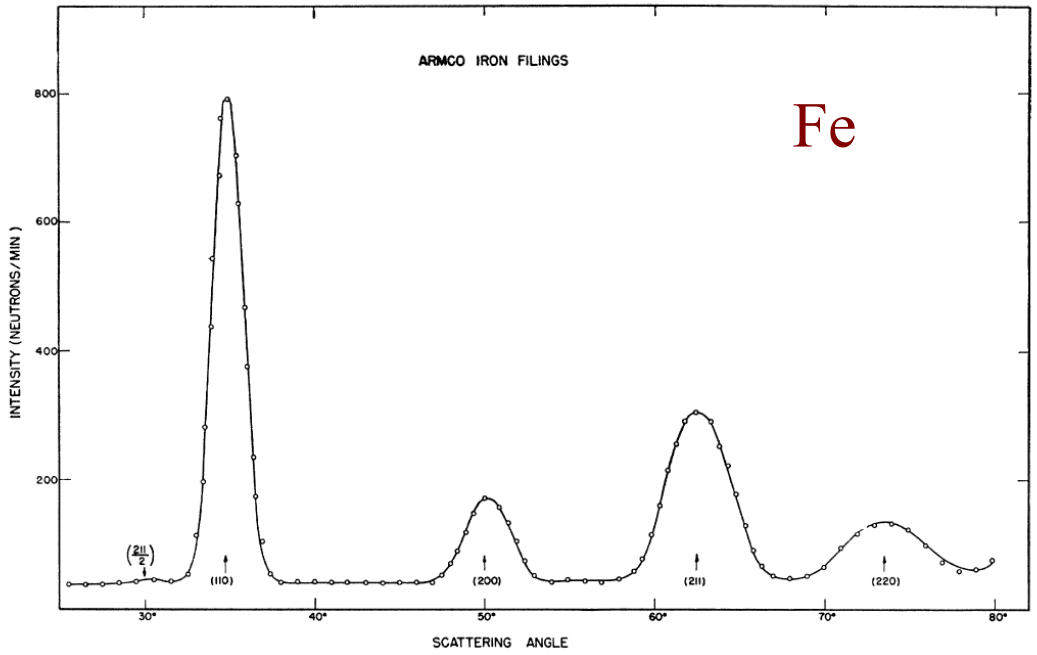

[Shull, Wollan, and Koehler, *PR* **84**, 912 (1951)]

Elastic peaks at multiples of the Bragg wavevector fix the magnetic distribution around each Fe site. But they provide no information about the individual interactions between the Fe spins.

2. The dynamical fingerprint of a spin state

By revealing how spins fluctuations are coupled, inelastic scattering *overdetermines* the spin state and interactions in any material.

Even these early inelastic measurements taken at ORNL's High Flux Isotope Reactor (HFIR) of the SW (spin-wave) spectrum $\omega(\mathbf{k})$ of Fe provide a great deal of information.

With the Heisenberg Hamiltonian

$$H = -\frac{1}{2}\sum_{i \neq j} J_{ij}\mathbf{S}_i \cdot \mathbf{S}_j \ ,$$

the SW stiffness is $D = 2J_1Sa^2$.

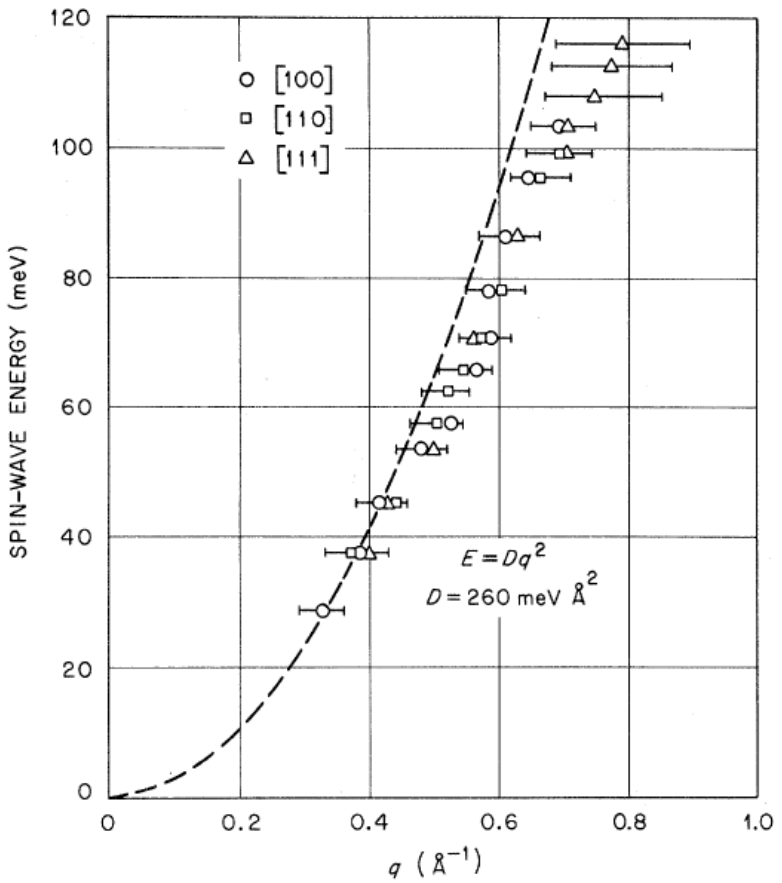

[Mook and Nicklow, *PRB* **7**, 336 (1973)]

2. The dynamical fingerprint of a spin state

By revealing how spins fluctuations are coupled, inelastic scattering *overdetermines* the spin state and interactions in a material.

Much more information is provided by the inelastic spectra of Ga-doped $CuFeO_2$ recently taken at ORNL's Spallation Neutron Source (SNS).

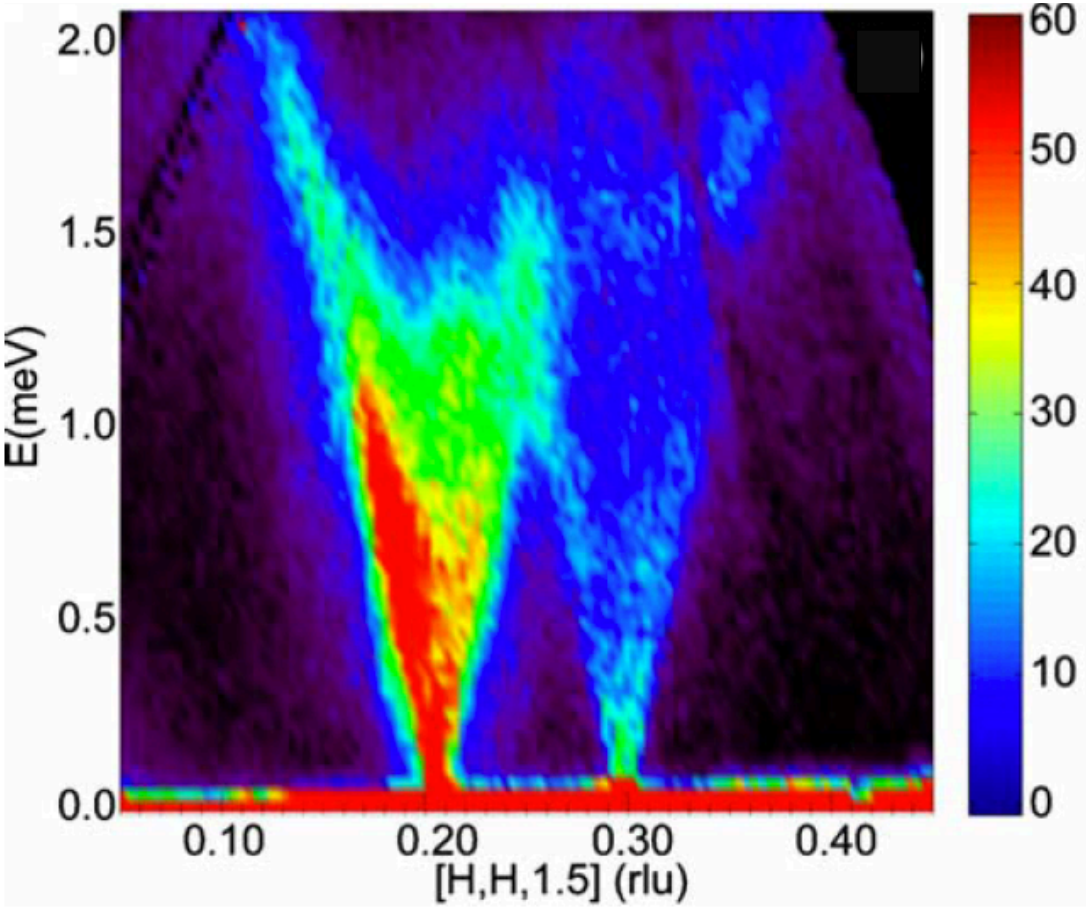

The inelastic spectra of a material provides its dynamical *fingerprint*. To extract information from that fingerprint, we follow the procedure:

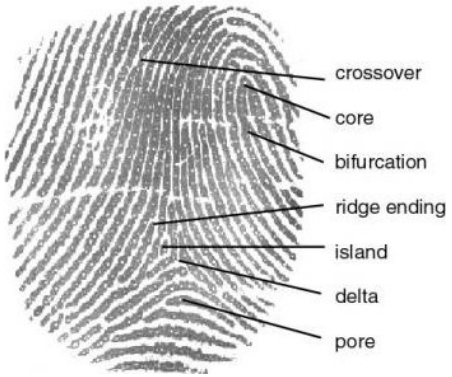

(1) Construct a trial spin state.

(2) Minimize the energy E for a given set of *interaction* parameters to determine the *variational* parameters of the trial spin state.

(3) Calculate the SW spectrum $\omega(\mathbf{k})$ and weights for that spin state.

(4) After folding in the instrumental resolution and magnetic form factor, compare the predicted and measured inelastic spectra $S(\mathbf{k}, \omega)$.

(5) Revise the *interaction* parameters as necessary and repeat steps (2-4) until the predicted and measured spectra agree.

A flow chart for this procedure is given below. Up till now, the comparison between $S(\mathbf{k}, \omega)_{exp}$ and $S(\mathbf{k}, \omega)_{pred}$ has been done visually!

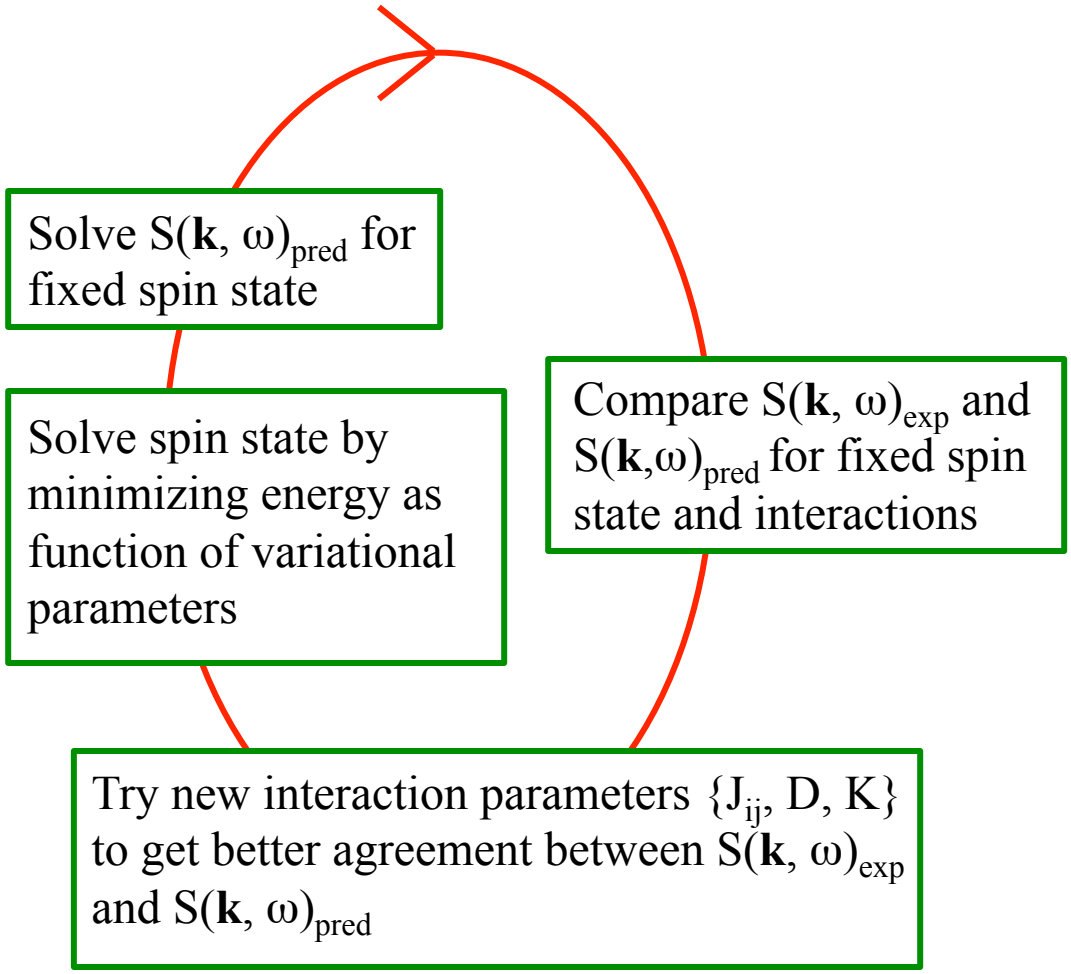

3. Multiferroic Materials

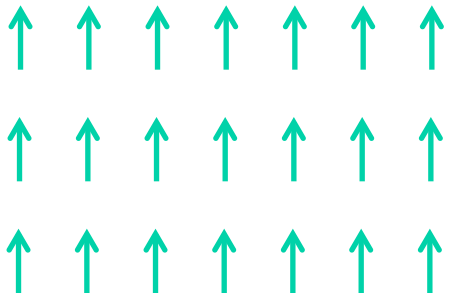

A FM develops a spontaneous magnetization **M** in the absence of an external magnetic field.

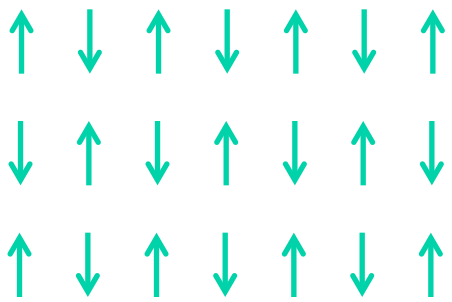

An antiferromagnet (AF) develops a spontaneous staggered magnetization in the absence of an external staggered magnetic field.

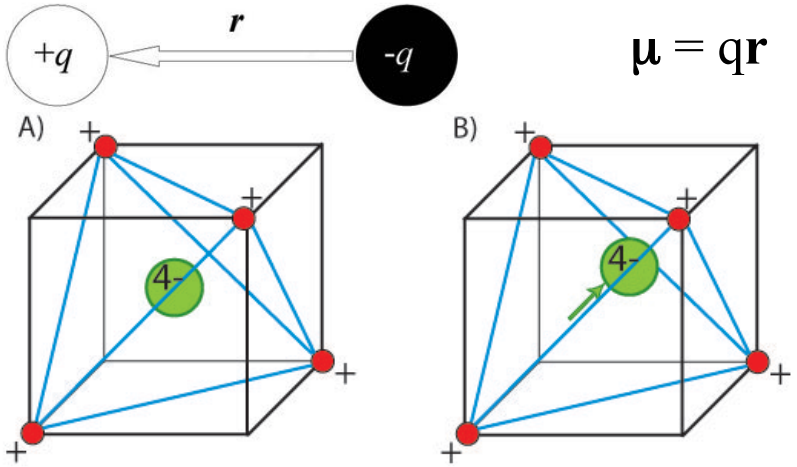

$\boldsymbol{\mu} = q\mathbf{r}$

Electric polarization: $\mathbf{P} = \Sigma_i \boldsymbol{\mu}_i$

A ferroelectric (FE) develops a spontaneous electric polarization **P** in the absence of an external electric field.

A material that has both FE and magnetic (FM or AF) properties is *multiferroic*. For these materials, **P** can be controlled by a magnetic field **H** and magnetism can be controlled by an electric field **E**.

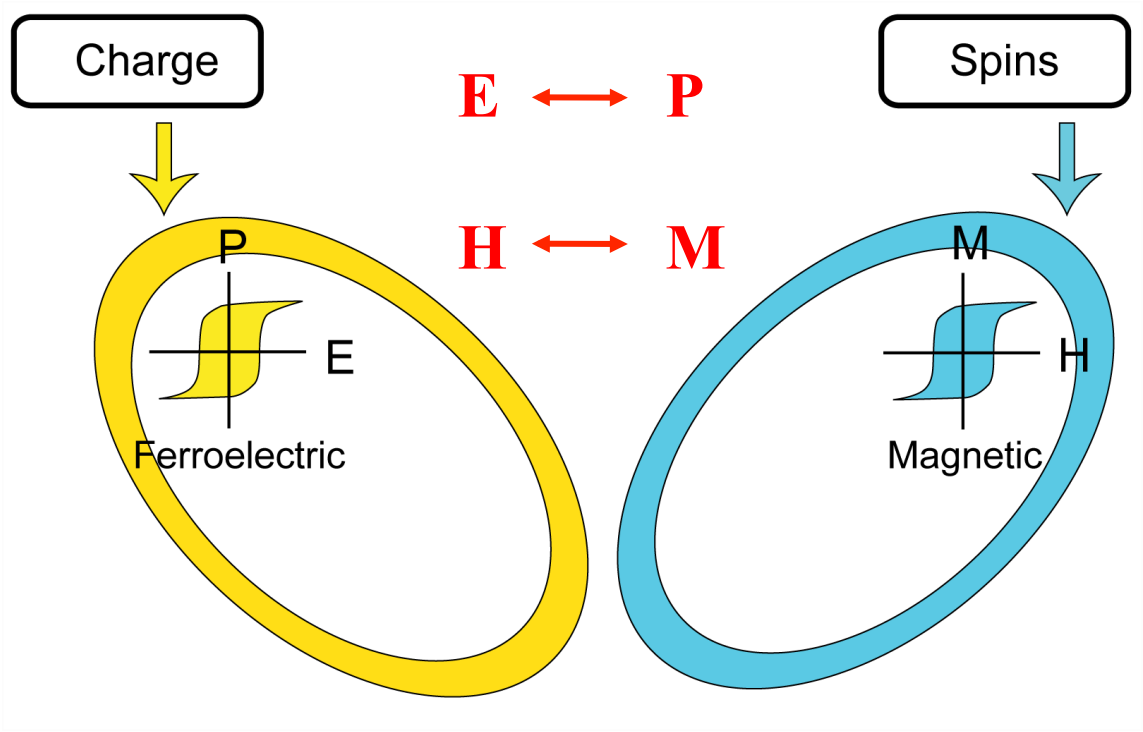

A material that has both FE and magnetic (FM or AF) properties is *multiferroic*. For these materials, **P** can be controlled by a magnetic field **H** and magnetism can be controlled by an electric field **E**.

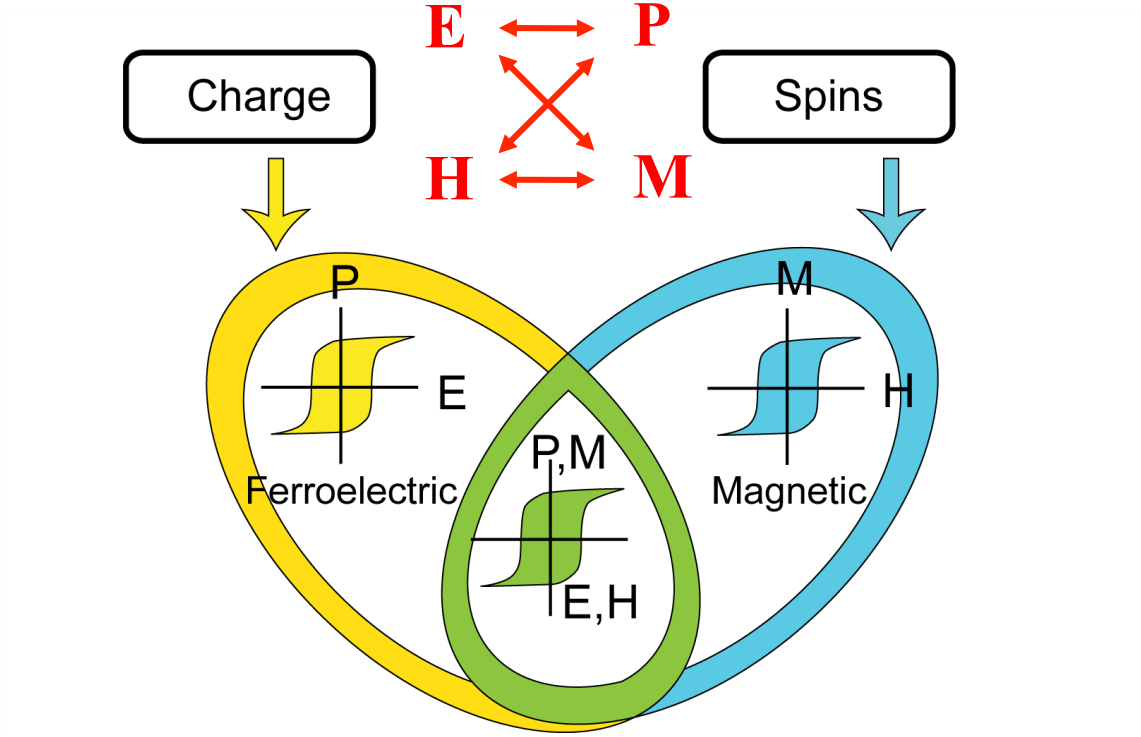

Two types of spin states are associated with multiferroic behavior:

1. A *spiral* is a chiral state where the plane of the spins is perpendicular to the propagation direction.

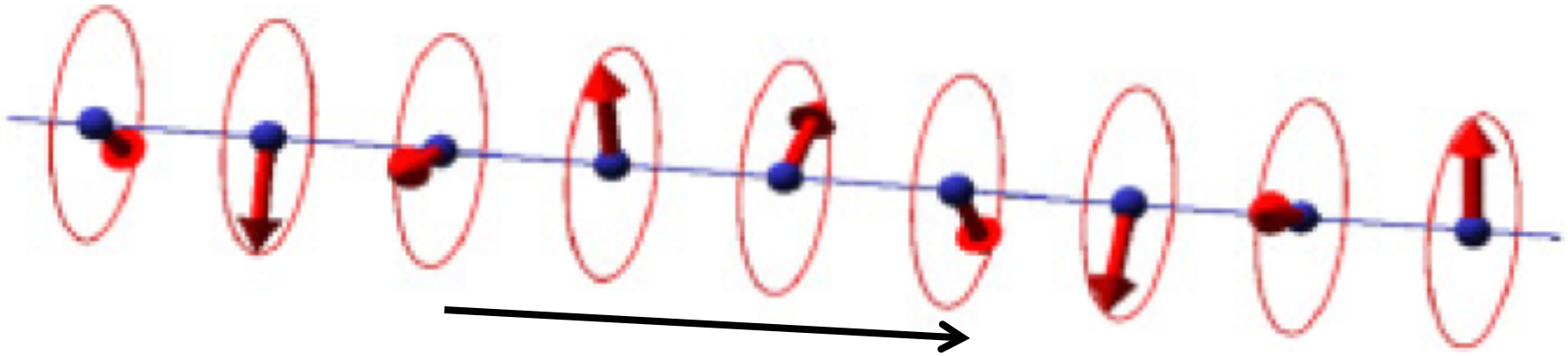

2. A *cycloid* is a chiral state where the plane of the spins contains the propagation direction.

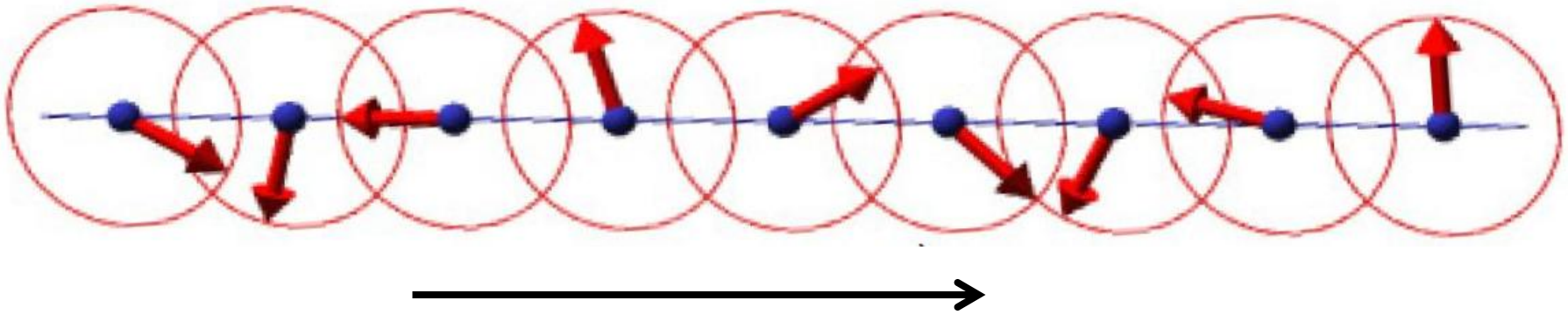

In Type I multiferroics, the FE transition temperature T_c is higher than the magnetic transition temperature T_N. Although T_N is high, the coupling between **P** and the cycloid is *weak*.

In Type II multiferroics, magnetic order induces **P** so that $T_N = T_c$. Although the coupling between **P** and the spiral or cycloid is *strong*, T_N is low.

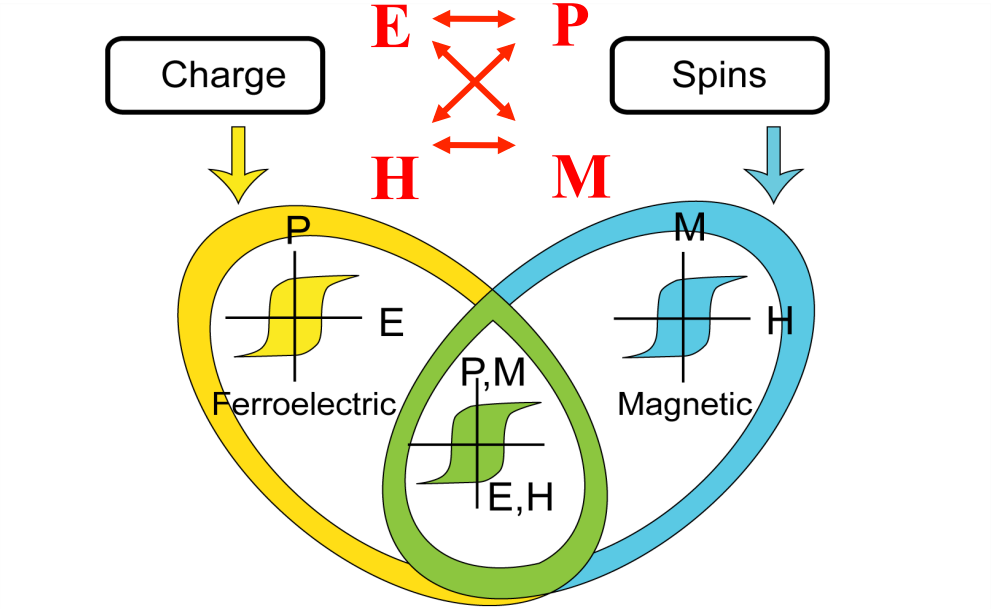

4. A Type II multiferroic: $CuFeO_2$

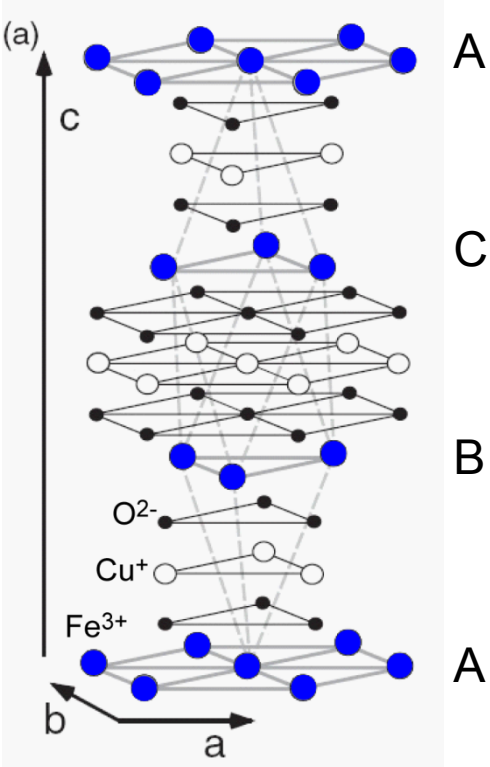

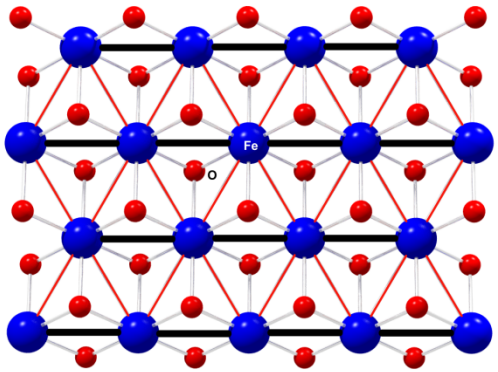

$CuFeO_2$ contains hexagonal planes of $S = 5/2$ Fe^{3+} ions stacked in an ABC pattern. Because the field H induces **P** together with the spiral, $CuFeO_2$ is a Type II multiferroic.

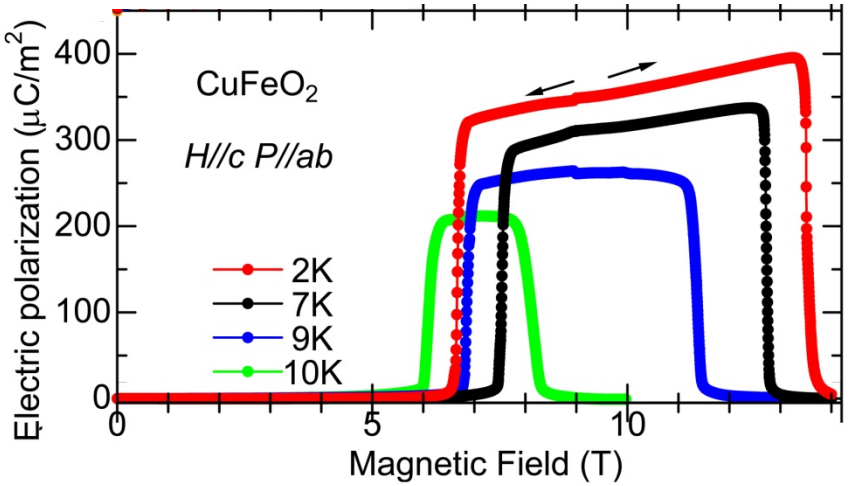

[Kimura *et al.*, *PRB* **73**, 220401 (2006)]

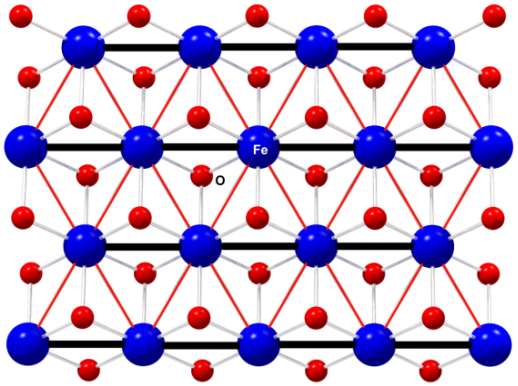

The AF interactions $J_1 < 0$ between the S = 5/2 spins are *geometrically frustrated* within each hexagonal plane.

Geometric frustration means that no spin state satisfies all the AF interactions.

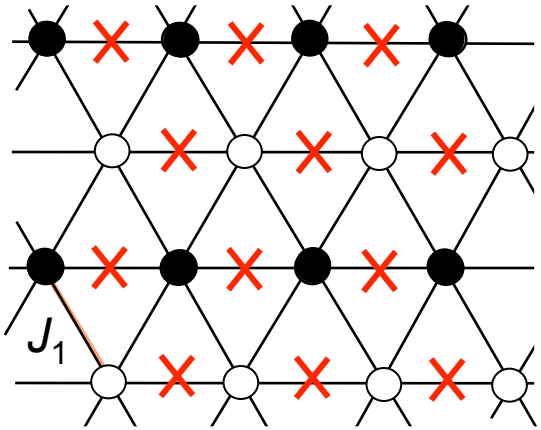

● down spin
○ up spin

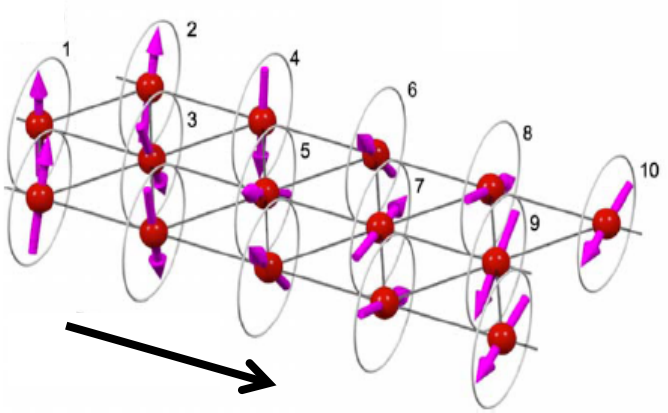

In Type II multiferroics, frustration produces a spiral or cycloid that breaks inversion symmetry. Broken inversion symmetry induces atomic displacements associated with **P**.

The spiral and polarization of $CuFeO_2$ are produced either by a magnetic field or by doping. In both cases, the spiral is preceded by an AF phase with spins aligned along the *c* axis.

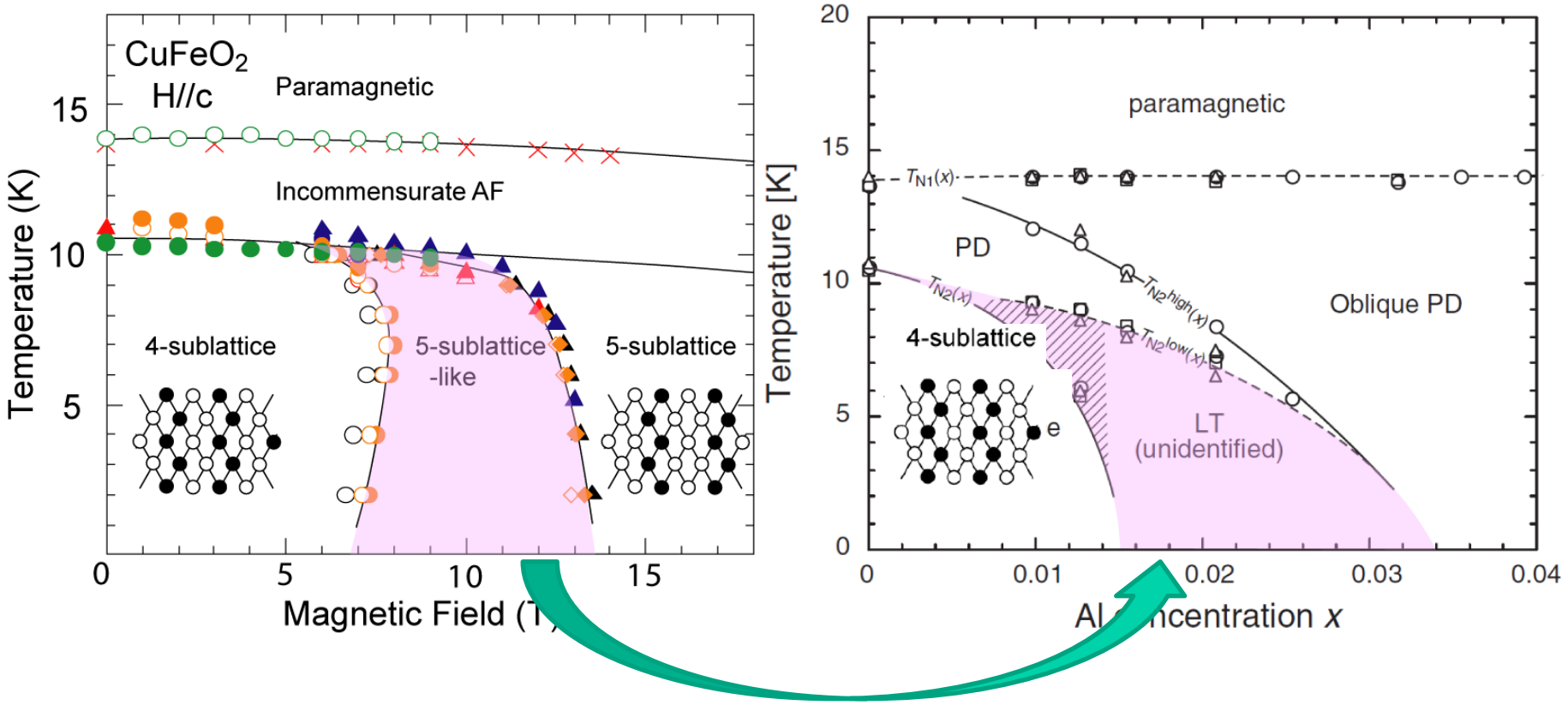

[Kimura *et al.*, *PRB* **73**, 220401 (2006)] [Terada *et al.*, *JPSJ* **74**, 2604 (2005)]

The symmetry of each hexagonal plane is broken by displacements of the oxygen atoms with period a**x** or wavevector 2π**x**/a.

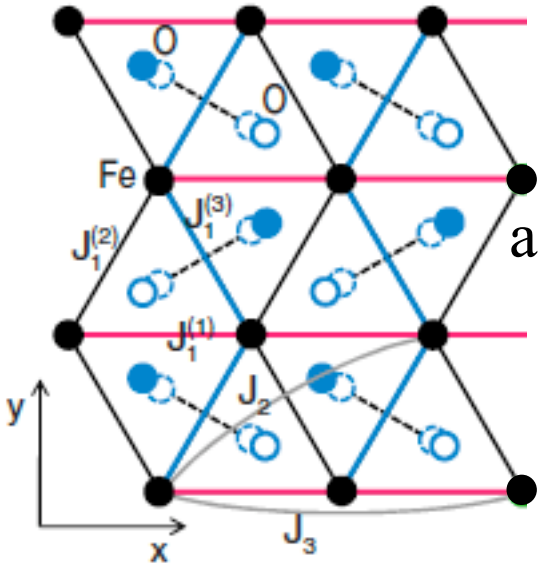

a = 3.03 Å

So the nearest-neighbor interactions become:

$$J_1^{(1)} = J_1^{(2)} = J_1 - O_1/2$$
$$J_1^{(3)} = J_1 + O_1$$

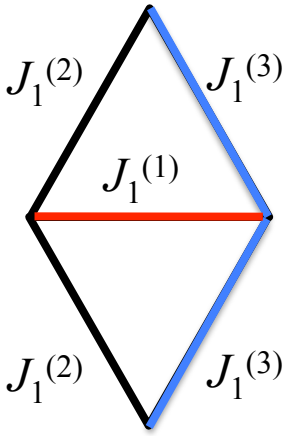

[Terada *et al.*, *JPSJ* **75**, 023602 (2006)]

The Hamiltonian of $CuFeO_2$ includes exchange interactions J_{ij} and easy-axis anisotropy K that aligns the spins along the c axis:

$$H = -\frac{1}{2}\sum_{i\neq j} J_{ij}\mathbf{S}_i \cdot \mathbf{S}_j - K\sum_i S_{iz}^2$$

For a given set of exchange interactions and anisotropy, the energy E is minimized using the trial spin state:

$$S_z(\mathbf{R}) = A\Big\{\sum_{l=0} C_{2l+1}\cos[Q(2l+1)\cdot x] - \sum_{l=0} B_{2l+1}\sin[(2\pi/a - Q)(2l+1)\cdot x]\Big\},$$

$$S_y(\mathbf{R}) = \sqrt{S^2 - S_z(\mathbf{R})^2}\,\mathrm{sgn}(\mathrm{g}(\mathbf{R})),$$

$$\mathrm{g}(\mathbf{R}) = \sin(Q\cdot x) + G_1\cos[(2\pi/a - Q)\cdot x]$$

[Fishman and Okamoto, *PRB* **81**, 020402 (2010);
Haraldsen *et al., PRB* **82**, 020404 (2010)]

Without the lattice distortion, only odd harmonics of **Q** would be needed and $B_{2l+1} = G_1 = 0$. Due to the lattice distortion, we must also include odd harmonics of $2\pi\mathbf{x}/a - \mathbf{Q}$.

In practice, only C_1, C_3, C_5, B_1, and B_3 are significant and $G_1 = -B_1/C_1$. So there are 6 variational parameters including Q.

Compare the predicted and measured excitation spectra S(**k**, ω) for Ga-doped $CuFeO_2$ along (H, H, 3/2):

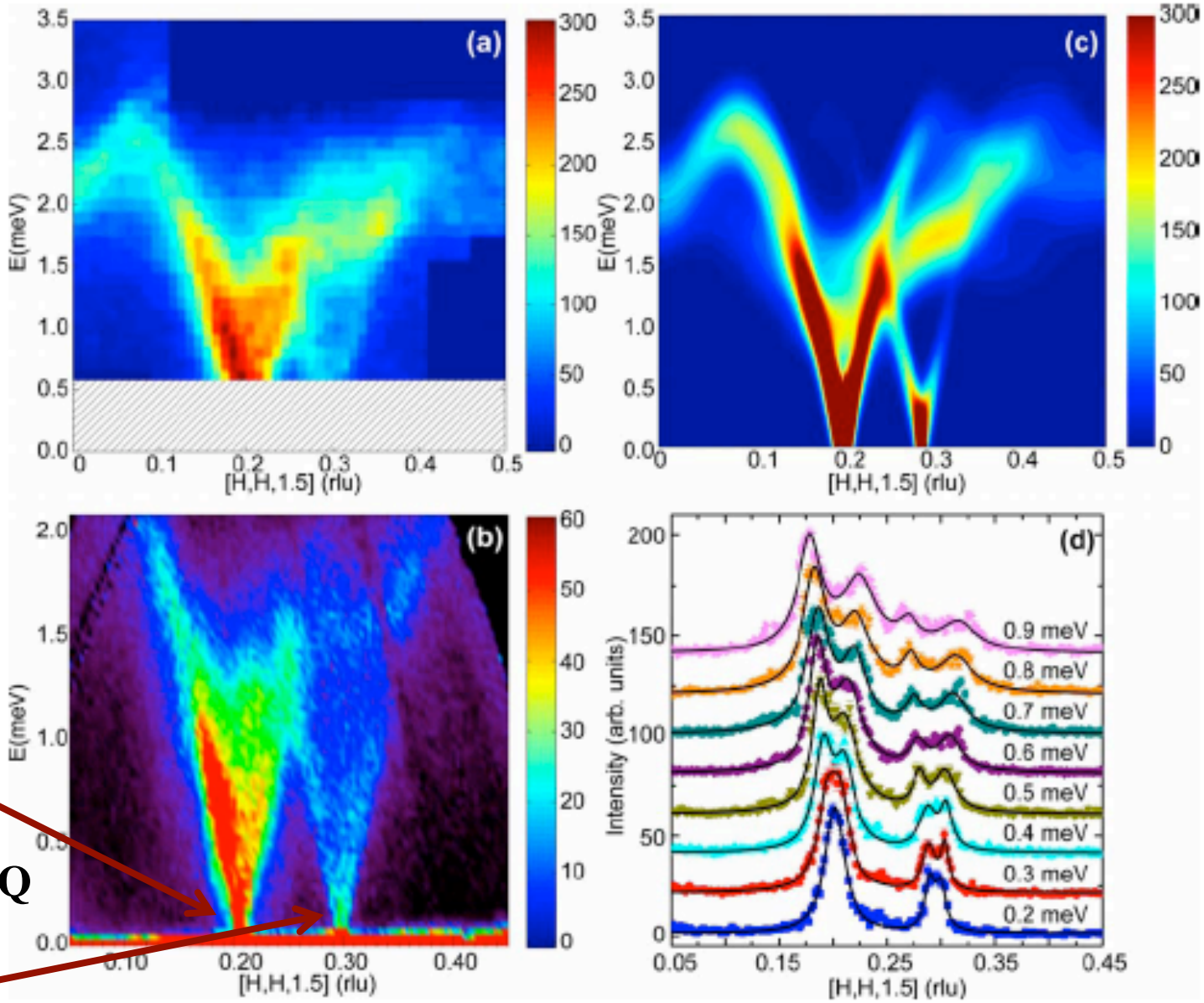

C_1 peak at **Q**

B_1 peak at $2\pi\mathbf{x}/a - \mathbf{Q}$ produced by the lattice distortion

And along (0.2, 0.2, L):

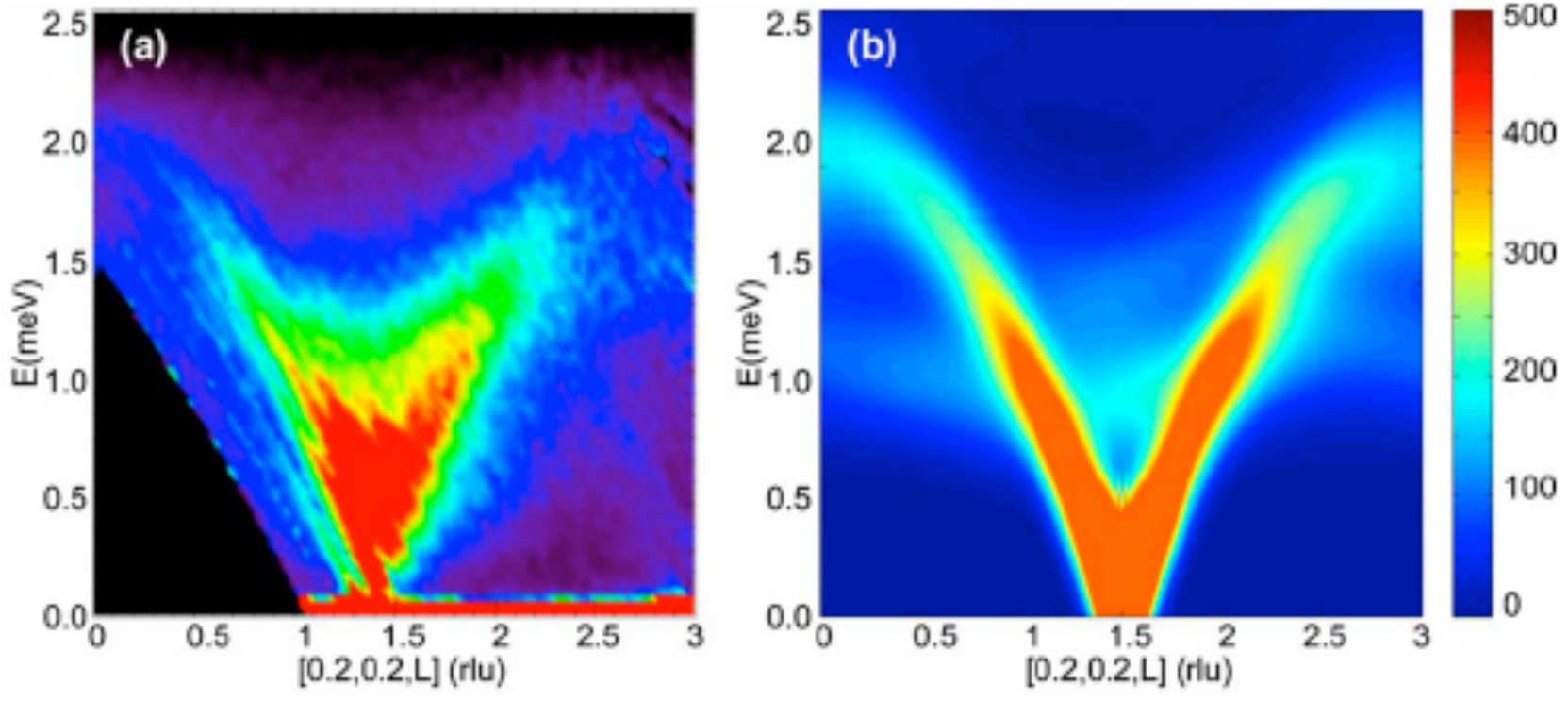

[Haraldsen, Ye, Fishman, Fernandez-Baca, Yamaguchi, Kimura, and Kimura, *PRB* **82**, 020404 (2010)]

A zero-frequency mode with wavevector (0.207, 0.207, 3/2) appears in the predicted $S(\mathbf{k}, \omega)$ because a spin rotation about the *c* axis does not cost energy.

Due to the remarkable agreement between the measured and predicted inelastic spectra, we are confident that we have correctly identified the FE spin state. The exchange interactions in pure and doped $CuFe_{1-x}Ga_xO_2$ are given below in meV.

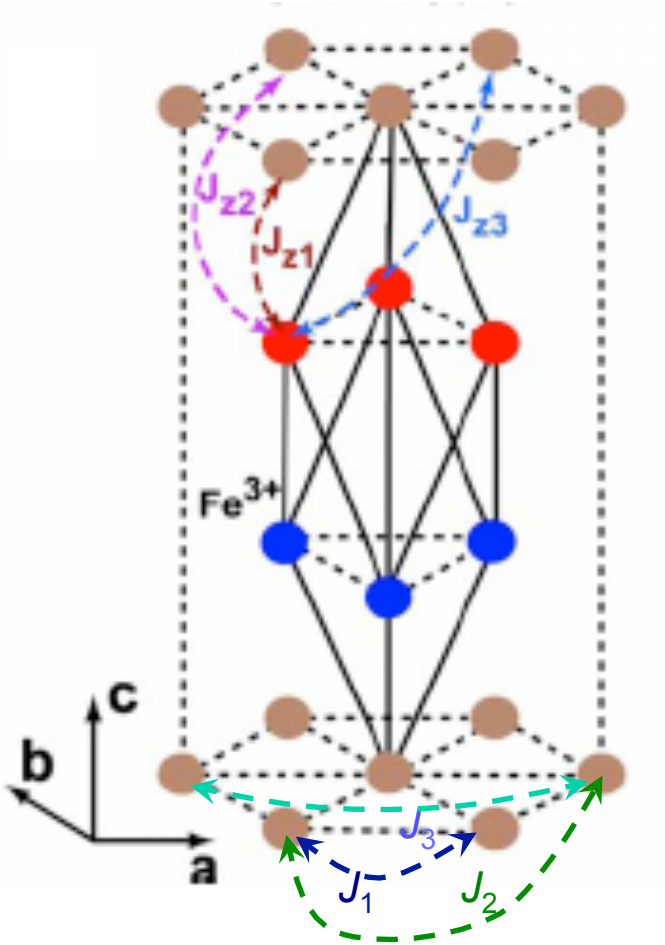

x	J_1	J_2	J_3	J_{z1}	J_{z2}	J_{z3}	K	O_1
0	−0.23	−0.12	−0.16	−0.06	0.07	−0.05	0.22	--
0.035	−0.19	−0.10	−0.13	−0.05	0.02	−0.01	0.01	0.07

The dominant effect of Ga doping is to reduce K from 0.22 to 0.01 meV while lowering the exchange interactions J_n and J_{zn} by about 20%.

Due to the remarkable agreement between the measured and predicted inelastic spectra, we are confident that we have correctly identified the FE spin state. The exchange interactions in pure and doped $CuFe_{1-x}Ga_xO_2$ are given below in meV.

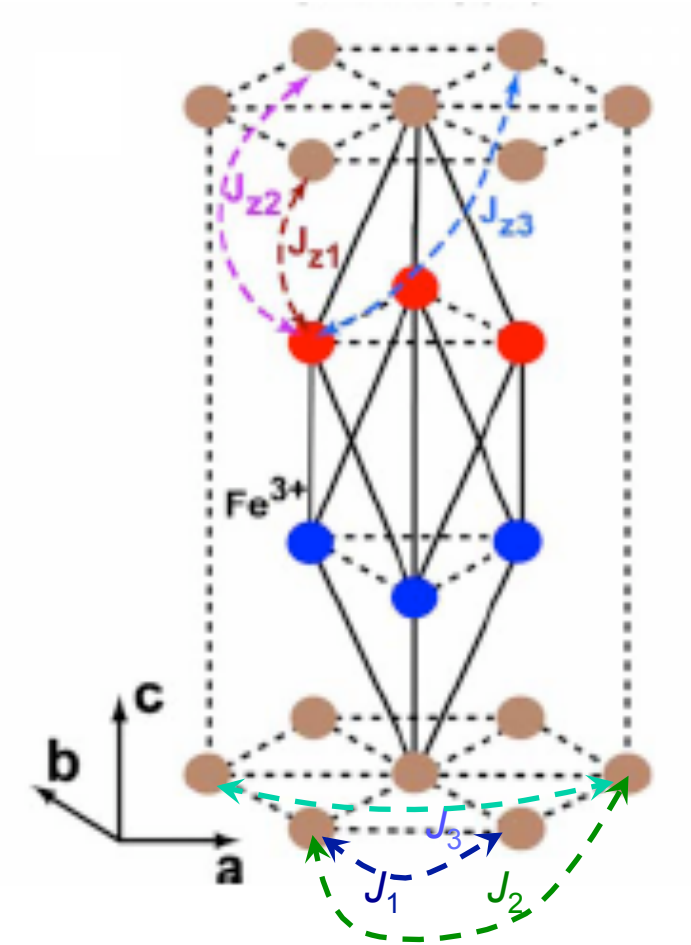

x	$J_2/\|J_1\|$	$J_3/\|J_1\|$	$J_{z1}/\|J_1\|$	$J_{z2}/\|J_1\|$	$J_{z3}/\|J_1\|$	$K/\|J_1\|$
0	−0.52	−0.70	−0.03	0.03	−0.02	0.96
0.035	−0.53	−0.68	−0.03	0.01	−0.005	0.005

The dominant effect of Ga doping is to reduce K from 0.22 to 0.01 meV while lowering the exchange interactions J_n and J_{zn} by about 20%.

The FE state is a distorted spiral with a distribution of turn angles:

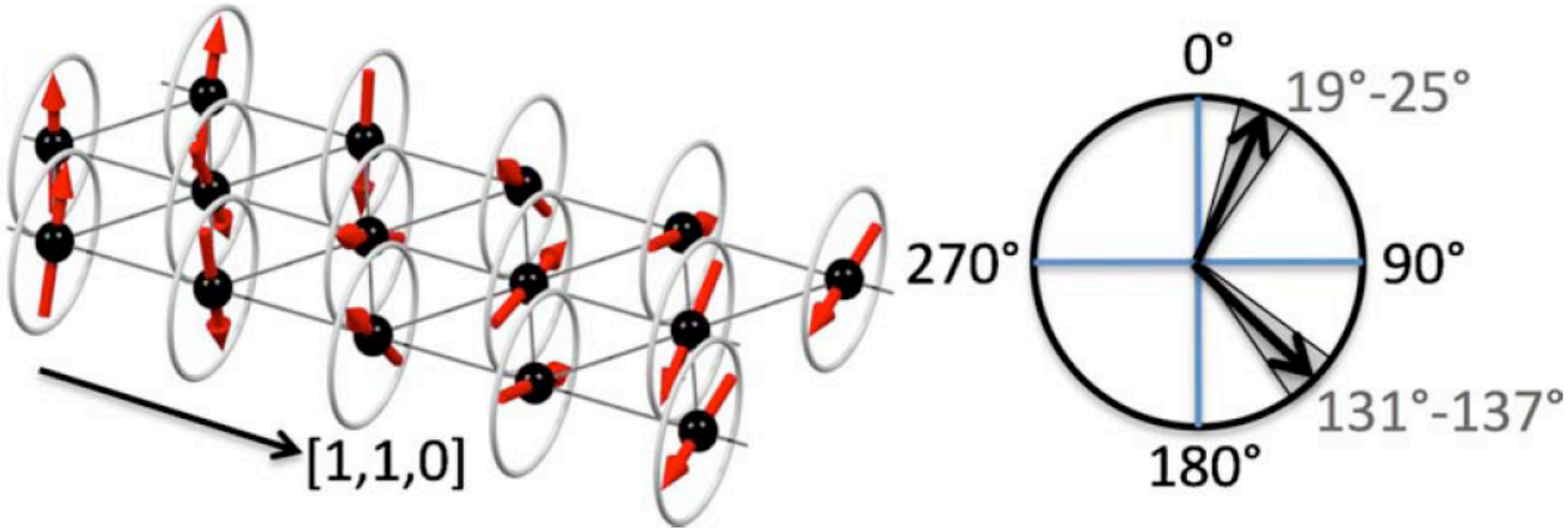

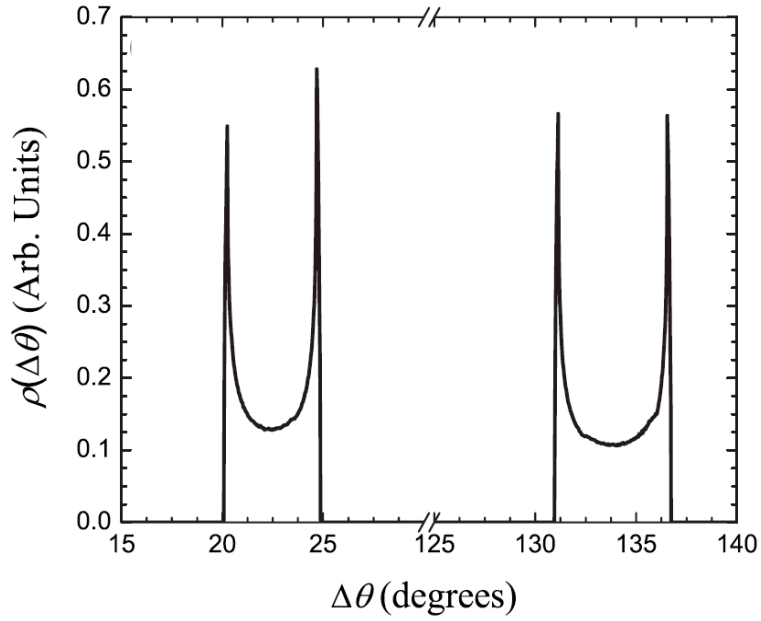

[Haraldsen and Fishman, *PRB* **82**, 144441 (2010)]

The two dominant turn angles (22º and 133º) are caused by the **Q** and $2\pi\mathbf{x}/a - \mathbf{Q}$ harmonics. The distributions about those angles are produced by higher harmonics.

5. A Type I multiferroic: $BiFeO_3$

$BiFeO_3$ is a Type I multiferroic with a FE transition at $T_c = 1100$ K and a magnetic transition at $T_N = 640$ K. It is the only known room temperature multiferroic. **P** is parallel to a cubic diagonal like **z**′.

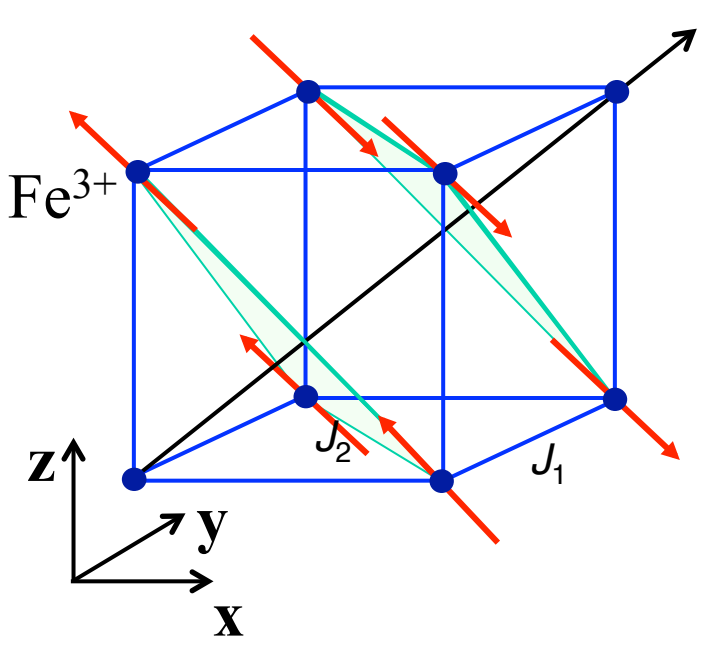

The AF exchange interactions between the S = 5/2 Fe^{3+} ions on the pseudo-cubic lattice are $J_1 < 0$ and $J_2 < 0$.

Without other interactions, J_1 and J_2 would produce a G-type AF.

In a Type I multiferroic, inversion symmetry is already broken by **P** below T_c. Produced by spin-orbit coupling, Dzyaloshinskii-Moriya (DM) interactions allow the spins to take advantage of this broken inversion symmetry.

The DM interaction **D** couples to the spin helicity $\mathbf{S}_i \times \mathbf{S}_j$. The electric polarization $\mathbf{P}^{ind}$ induced by the cycloid is parallel to **P**.

$$\mathbf{P}^{ind} \sim \mathbf{e}_{ij} \times (\mathbf{S}_i \times \mathbf{S}_j),$$

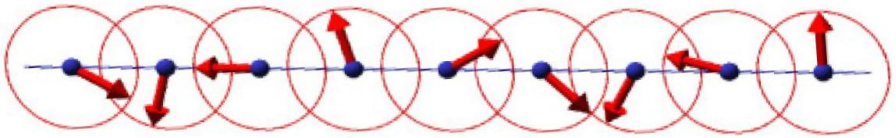

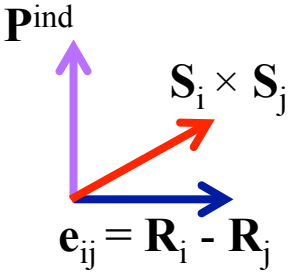

Because $|D| << |J_{ij}|$, the period of the cycloid in Type I multiferroics is typically very long. By contrast, the period of the spiral or cycloid in Type II multiferroics like $CuFeO_2$ is typically rather short.

Below T_N, the DM interaction *D* along **y**′ produces a cycloid with a period of $\lambda = a/(2^{1/2}\delta) = 62$ nm and wavevector

$$\mathbf{Q} = (2\pi/a)(0.5 + \delta, 0.5, 0.5 - \delta), \quad \delta = 0.0045 << 1$$

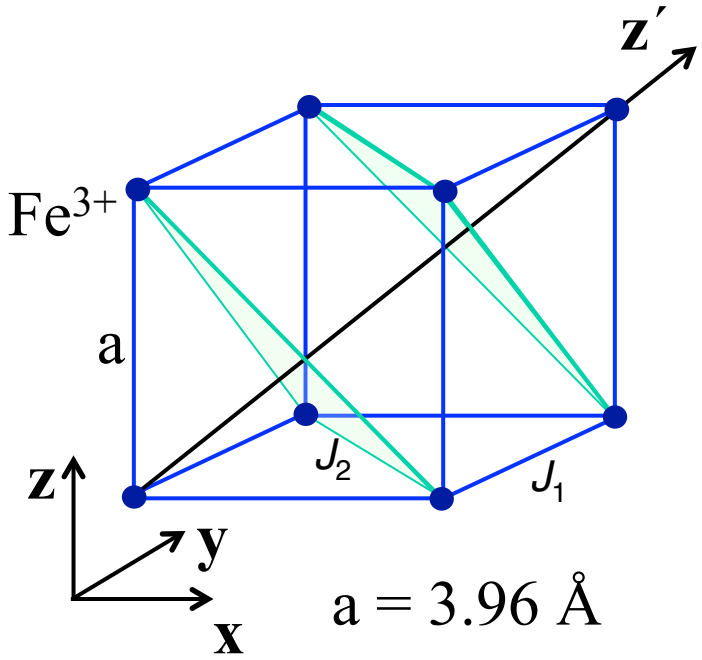

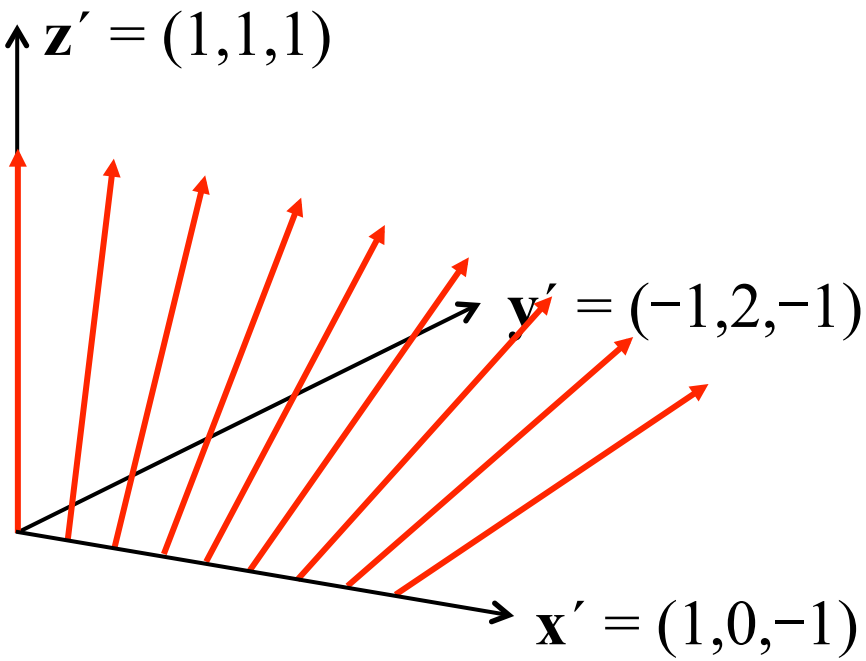

The spins lie predominantly in the *x*′*z*′ plane.

Another DM interaction D' along $\mathbf{z}'$ produces the weak FM moment perpendicular to $\mathbf{z}'$ in the AF phase above 19 T.

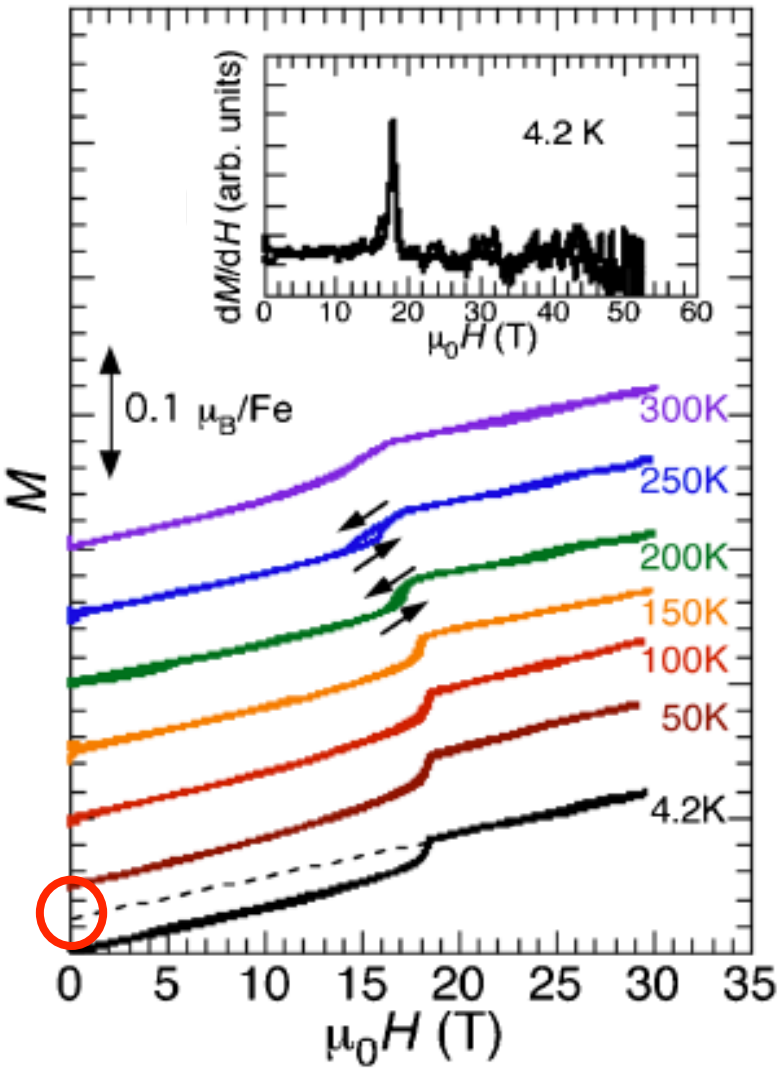

Projected onto the $x'y'$ plane, the extrapolated zero-field state is:

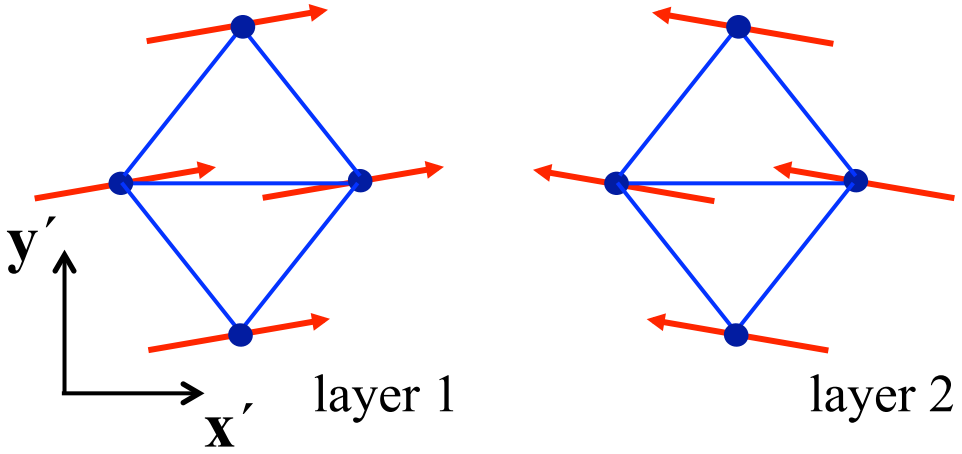

The zero-field moment $\mathbf{M}_0 = 0.03\mu_B\,\mathbf{y}'$ corresponds to $D' = 0.054$ meV.

[Tokunaga, Azuma, and Shimakawa, *JPSJ* **79**, 064713 (2010)]

In the multiferroic phase, D' tilts the cycloid out of the $x'z'$ plane.

The tilt changes sign from one hexagonal layer to the next.

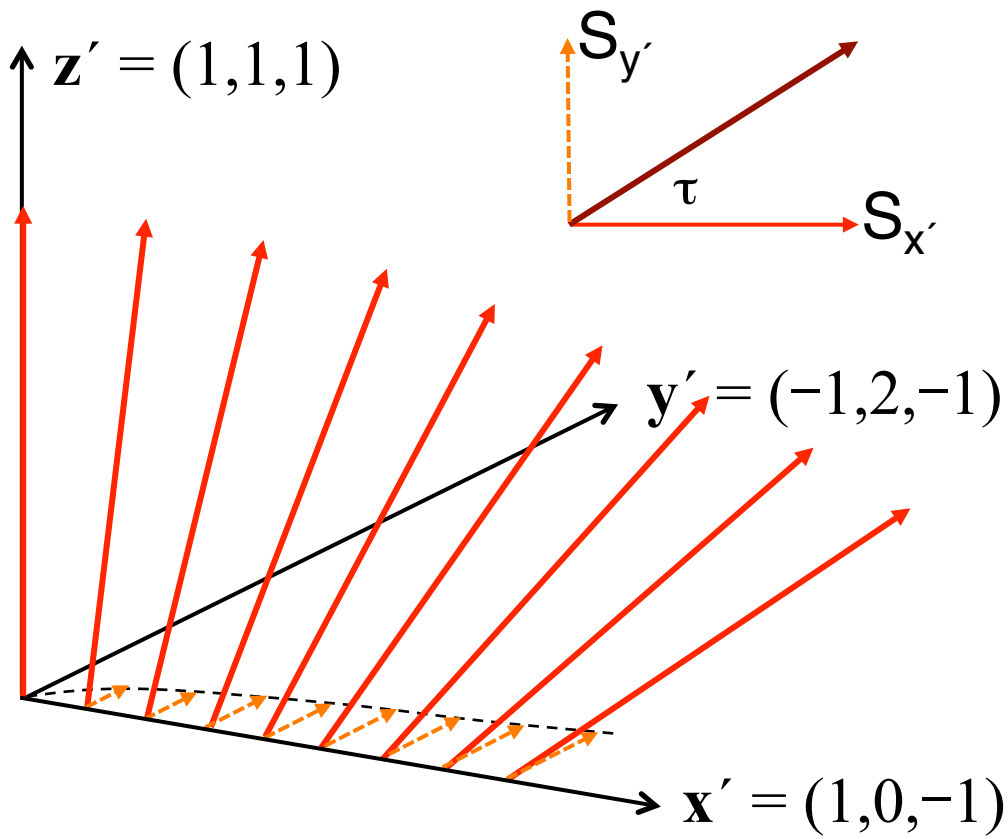

The *maximum* cycloidal spin S_0 along $\mathbf{y}'$ equals $M_0/2\mu_B = 0.015$ where M_0 is the weak FM moment of the AF phase: $S_0 = 0.015$ implies $\tau = 0.34^o$.

In zero field, the Hamiltonian of $BiFeO_3$ is:

$$\mathcal{H} = -J_1 \sum_{\langle i,j \rangle} \mathbf{S}_i \cdot \mathbf{S}_j - J_2 \sum_{\langle i,j \rangle'} \mathbf{S}_i \cdot \mathbf{S}_j - K \sum_i (\mathbf{S}_i \cdot \mathbf{z}')^2$$
$$- \frac{D}{a\sqrt{2}} \sum_{\mathbf{R}_j = \mathbf{R}_i + \mathbf{e}_{ij}} (\mathbf{z}' \times \mathbf{e}_{ij}) \cdot (\mathbf{S}_i \times \mathbf{S}_j)$$
$$- D' \sum_{\mathbf{R}_j = \mathbf{R}_i + \mathbf{e}_{ij}} (-1)^{R_{iz'}/c} \mathbf{z}' \cdot (\mathbf{S}_i \times \mathbf{S}_j)$$

J_1 and J_2: AF exchange interactions.

$\mathbf{e}_{ij}$ = a**x**, a**y**, a**z** first neighbors

K: easy-axis anisotropy along **z**´.

D: DM interaction along **y**´ responsible for the cycloidal period $\lambda = a/(2^{1/2}\delta)$.

D´: DM interaction along **z**´ responsible for the cycloidal tilt τ and the weak FM moment of the AF phase.

The energy E is minimized using the trial spin state:

$$
\begin{aligned}
S_{x'}(\mathbf{R}) &= (-1)^{R_{z'}/c}\cos\tau\sqrt{S^2 - S_{z'}(\mathbf{R})^2} \\
&\quad \operatorname{sgn}\bigl(\sin(2\sqrt{2}\pi\delta R_{x'}/a)\bigr), \\
S_{y'}(\mathbf{R}) &= \sin\tau\sqrt{S^2 - S_{z'}(\mathbf{R})^2} \\
&\quad \operatorname{sgn}\bigl(\sin(2\sqrt{2}\pi\delta R_{x'}/a)\bigr), \\
S_{z'}(\mathbf{R}) &= (-1)^{R_{z'}/c} S \sum_{m=0}^{\infty} C_{2m+1}\cos\bigl((2m+1)2\sqrt{2}\pi\delta R_{x'}/a\bigr).
\end{aligned}
$$

Higher harmonics $C_{2m+1>1}$ are produced by either the easy-axis anisotropy K or the DM interaction D'. While K favors the antinodes of the cycloid with $\langle(S_{z'})^2\rangle > 1/2$, D' favors the nodes of the cycloid with $\langle(S_{z'})^2\rangle < 1/2$.

In practice, only C_1, C_3, and C_5 are significant. Since $C_1 + C_3 + C_5 = 1$, there are 4 variational parameters including τ and δ.

Inelastic neutron scattering measurements of the SW frequencies ω(**k**) can be used to obtain J_1 and J_2.

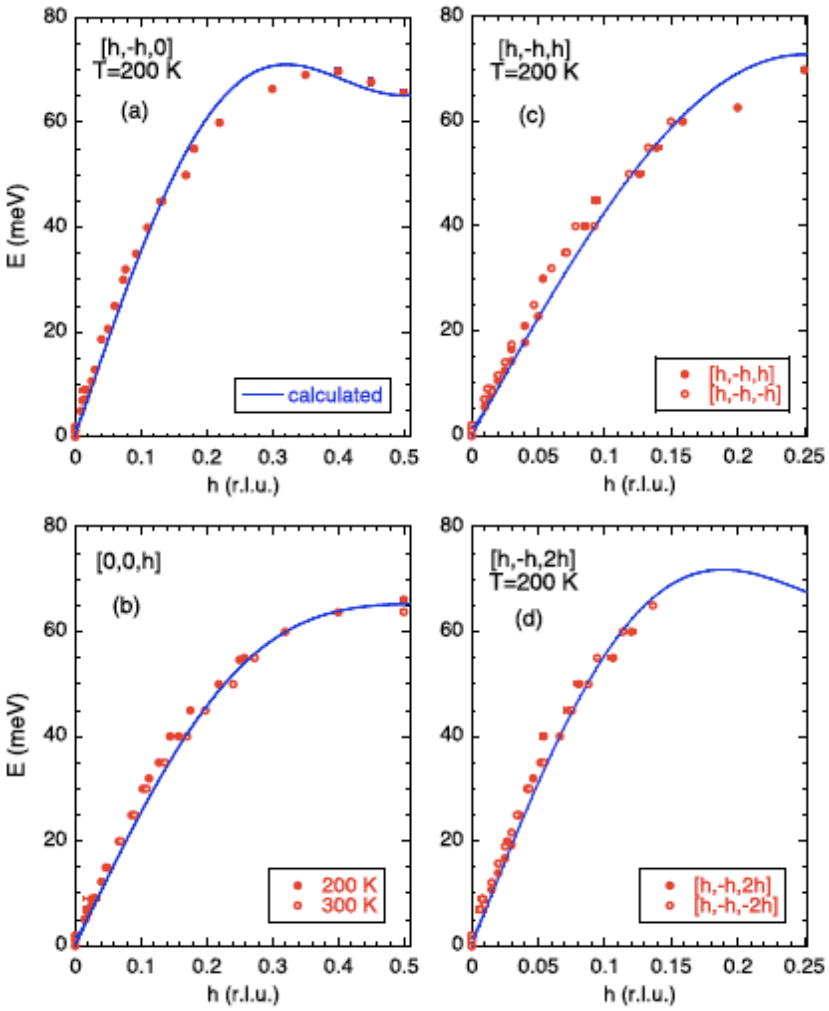

$J_1 = -4.5$ meV, $J_2 = -0.2$ meV

But the ordering wavevectors
Q = (2π/a)(0.5 ± δ, 0.5, 0.5 ∓ δ)
are too close together to accurately estimate the low-energy interactions D, D', and K.

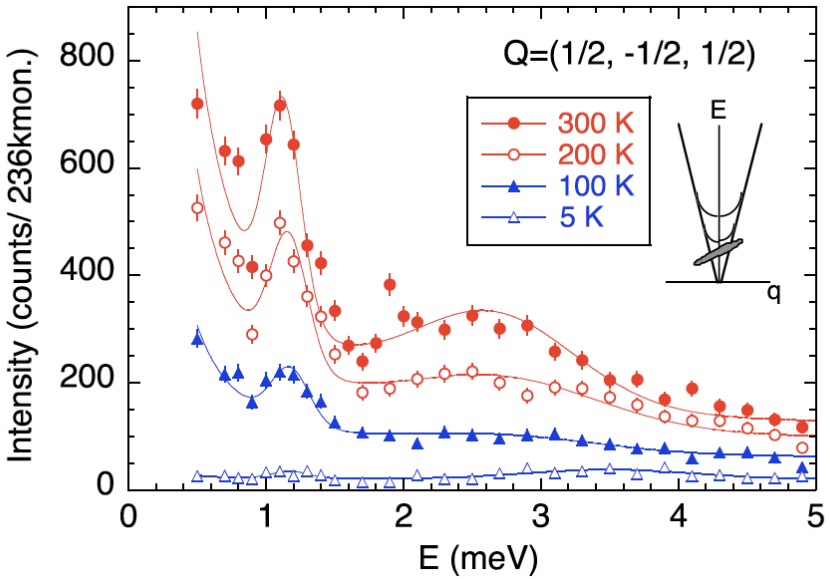

[Matsuda, Fishman, Hong, Lee, Ushiyama, Yanagisawa, Tomioka, and Ito, *PRL* **109**, 067205 (2012)]

Fortunately, Raman and THz spectroscopies provide the optically-active SW frequencies $\omega(\mathbf{Q})$ at the ordering wavevector. THz spectroscopy detected four modes in zero magnetic field.

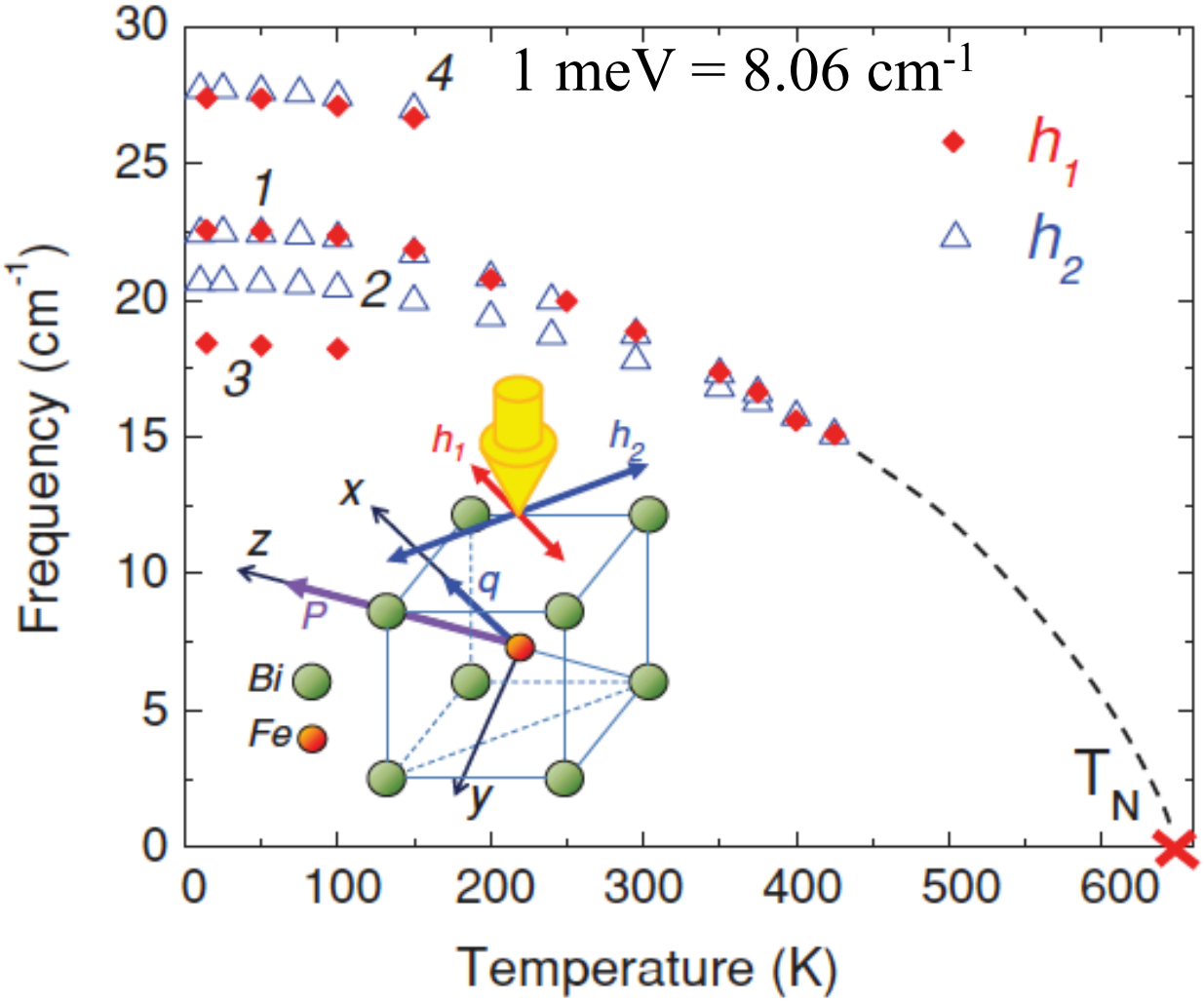

[Talbayev, Trugman, Lee, Yi, Cheong, and Taylor, *PRB* **83**, 094403 (2011)]

Fixing $S_0 = 0.015$, we compare the predicted and measured mode frequencies as a function of K (the only free parameter).

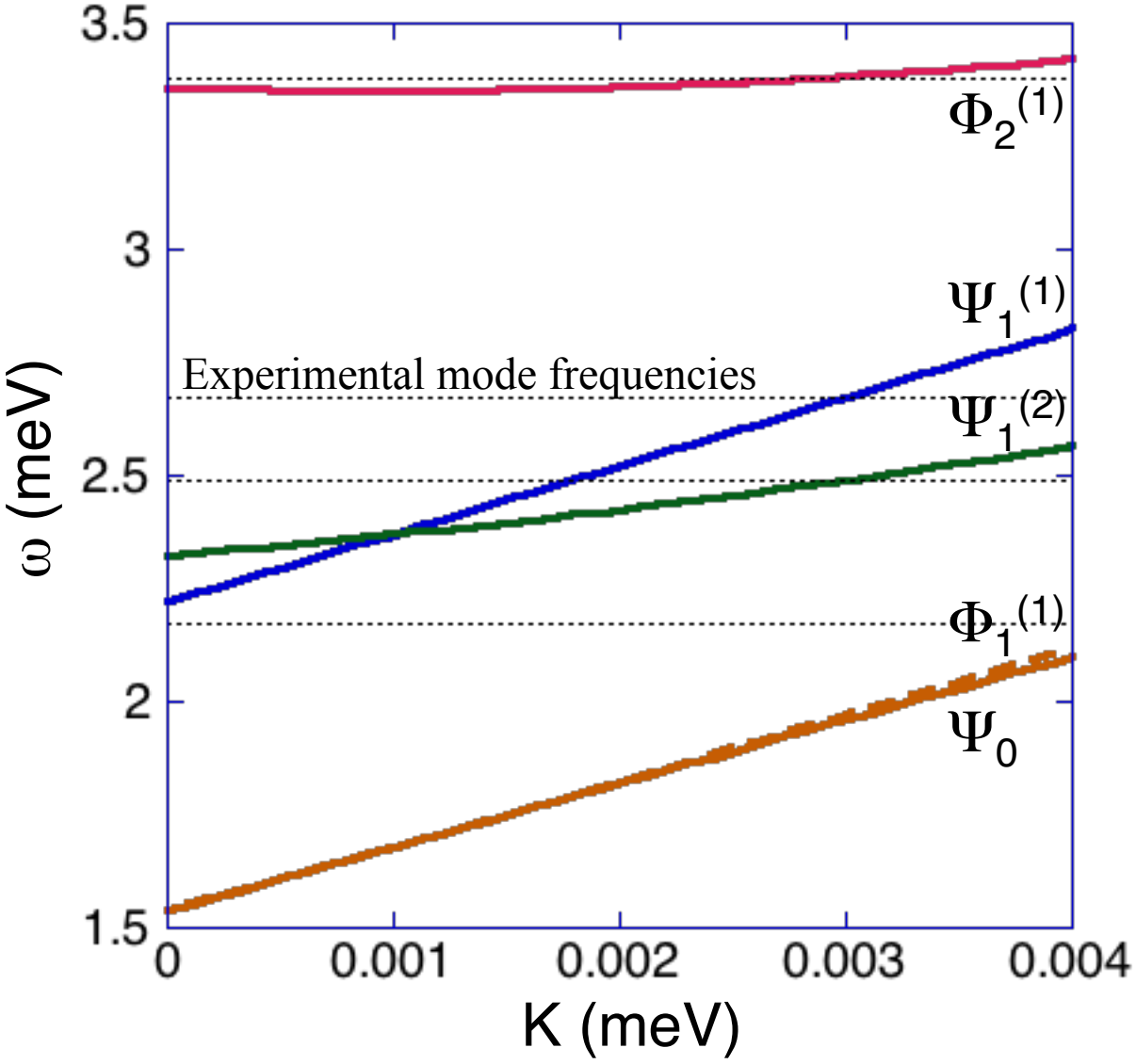

Φ_n modes are in the cycloidal plane.

Ψ_n modes are out of the cycloidal plane.

For n > 0, each mode is split by higher harmonics of the cycloid produced by either K or D'.

[Fishman, Furukawa, Haraldsen, Matsuda, and Miyahara, *PRB* **86**, 220402 (2012)]

Fixing $S_0 = 0.015$, we compare the predicted and measured mode frequencies as a function of K (the only free parameter).

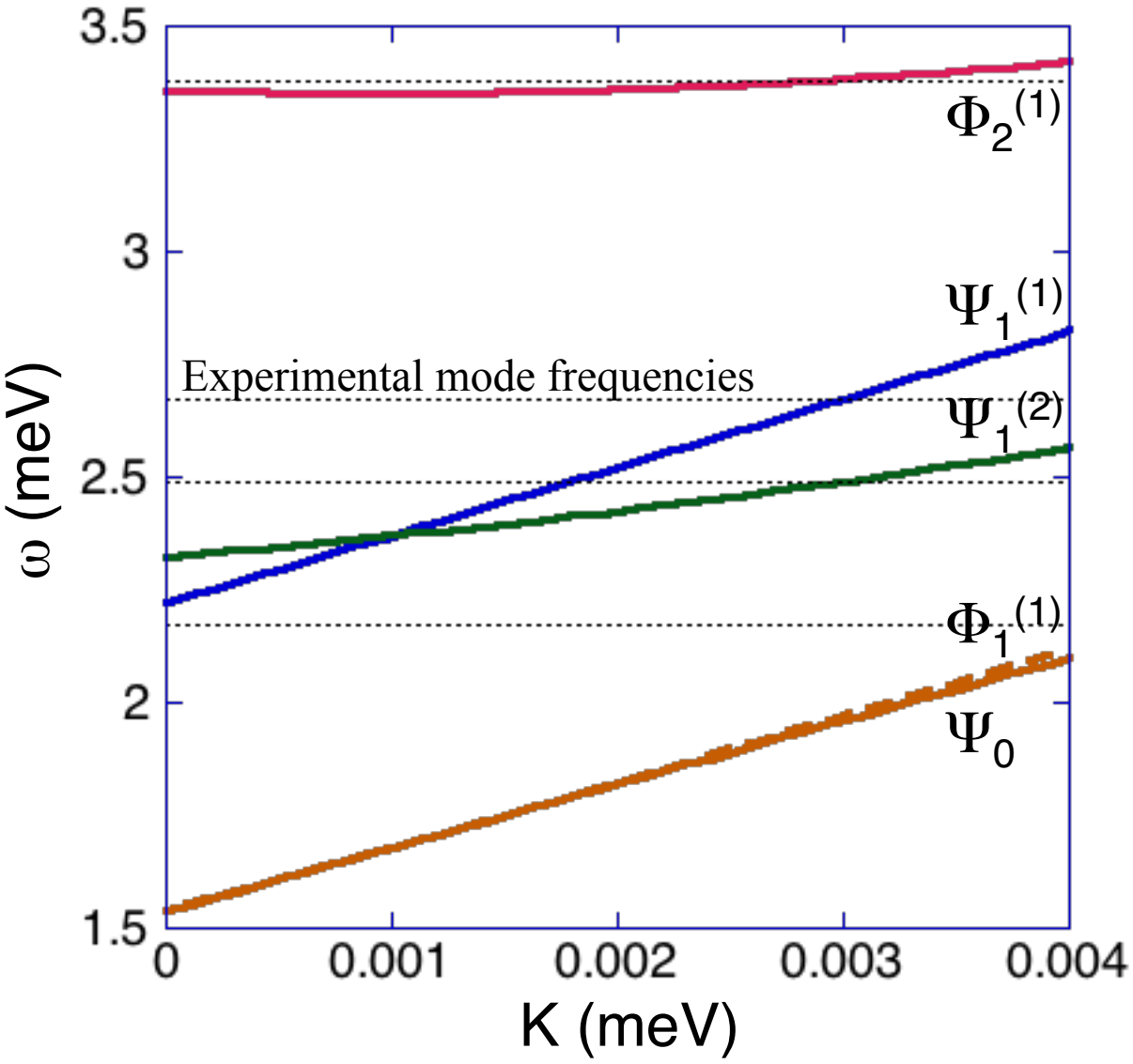

The nearly-degenerate $\Psi_0/\Phi_1^{(1)}$ modes are responsible for the low-frequency peak at 2.2 meV or 18 cm^{-1}. The best overall fit to the data is obtained with

$K = 0.0035$ meV
$D = 0.106$ meV
$D' = 0.054$ meV

[Fishman, Furukawa, Haraldsen, Matsuda, and Miyahara, *PRB* **86**, 220402 (2012)]

To confirm the interaction parameters and spin state, we examine the effect of a magnetic field. The three magnetic domains have different wavevectors $\mathbf{Q}_n$ and different coordinate systems:

domain 1: $\mathbf{x}' = (1,-1,0)$, $\mathbf{y}' = (1,1,-2)$
domain 2: $\mathbf{x}' = (1,0,-1)$, $\mathbf{y}' = (-1,2,-1)$
domain 3: $\mathbf{x}' = (0,1,-1)$, $\mathbf{y}' = (-2,1,1)$

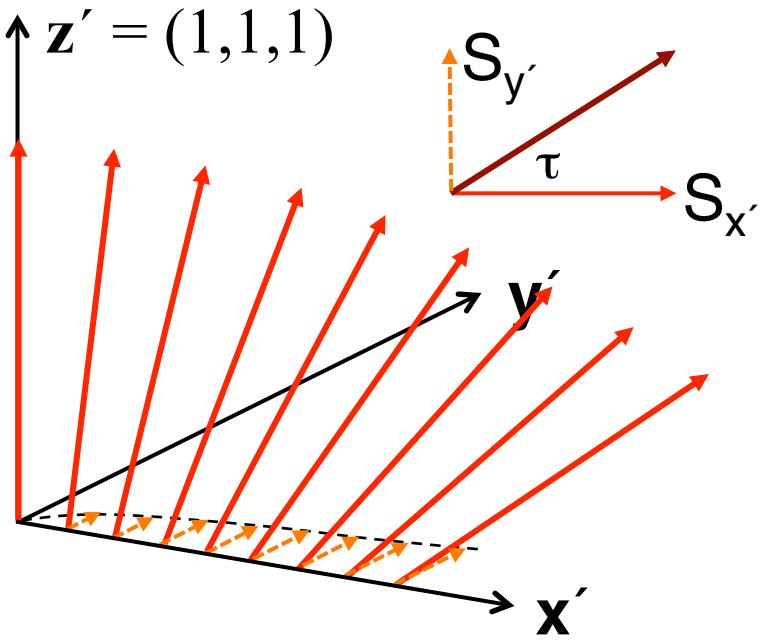

$$\mathbf{Q}_1 = (2\pi/a)(0.5 + \delta, 0.5 - \delta, 0.5)$$

$$\mathbf{Q}_2 = (2\pi/a)(0.5 + \delta, 0.5, 0.5 - \delta)$$

$$\mathbf{Q}_3 = (2\pi/a)(0.5, 0.5 + \delta, 0.5 - \delta)$$

In field $\mathbf{H} = H\mathbf{m}$ with $\mathbf{m} = (0,0,1)$, domains 2 and 3 have the same equilibrium and dynamical properties.

For **m** = (0,0,1), domain 1 with

$$\mathbf{Q}_1 = (2\pi/a)(0.5 + \delta, 0.5 - \delta, 0.5)$$

and spins primarily in the [−1,−1,2] plane has lower energy than domains 2 and 3.

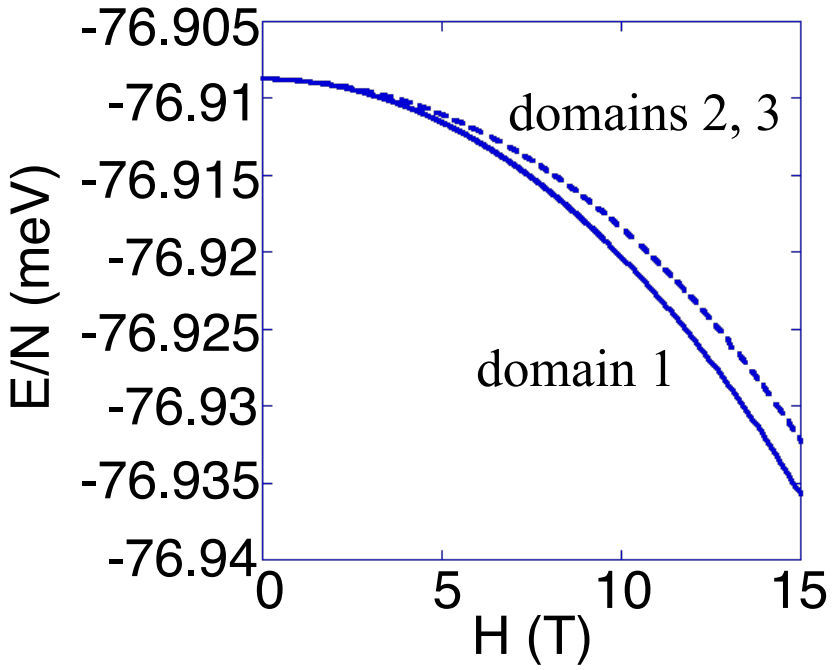

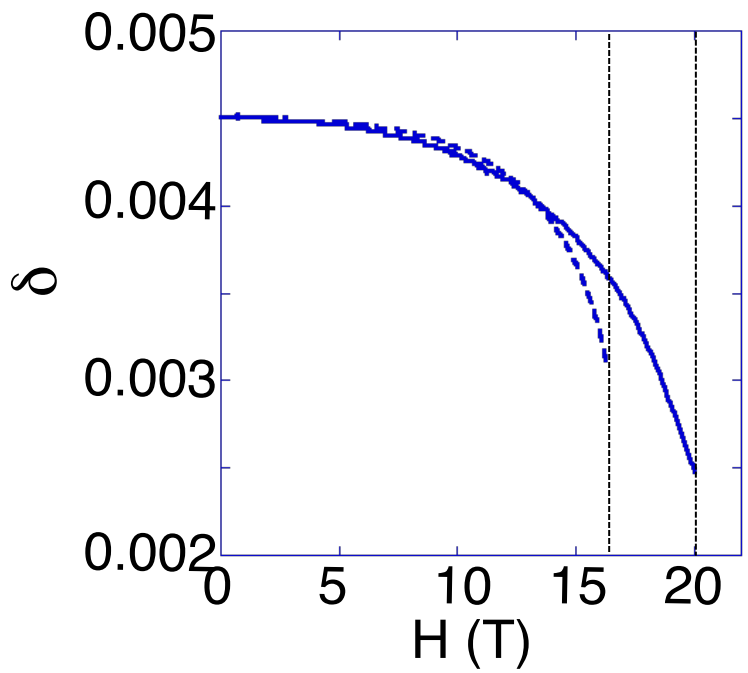

The predicted critical fields H_c = 16.2 and 20.1 T (above which the AF phase is stable) of the three domains are different.

Spectroscopy data was taken with **m** = (0,0,1) and two different THz fields:

$\mathbf{h}_1 = (1,-1,0)$, $\mathbf{e}_1 = (1,1,0)$ (circles)

$\mathbf{h}_2 = (1,1,0)$, $\mathbf{e}_2 = (1,-1,0)$ (triangles)

Due to the energy difference between domains, domains 2 and 3 are depopulated above 6 T, indicated by the dashed vertical line on the left.

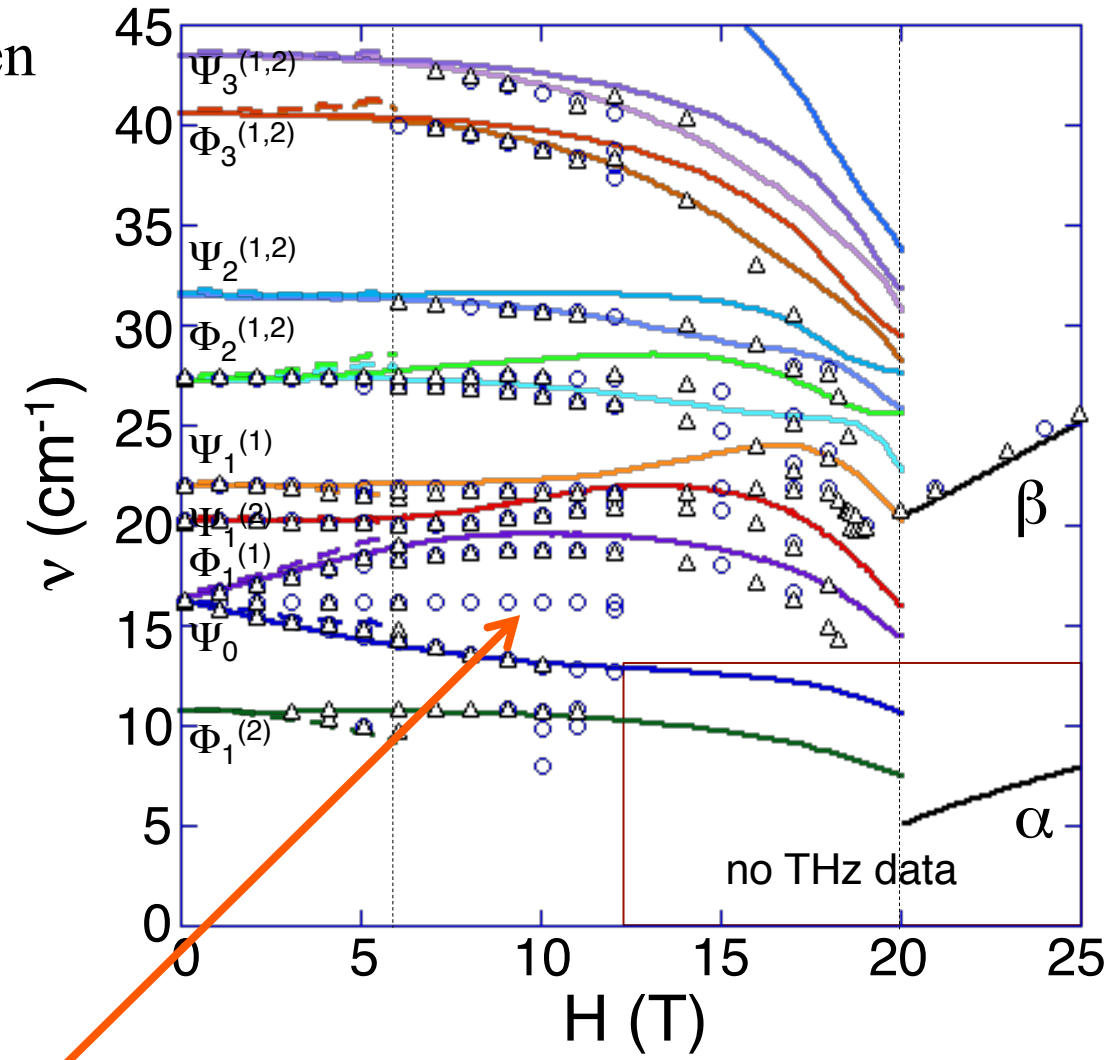

[Nagel, Fishman, Engelkamp, Talbayev, Yi, Cheong, and Rõõm, *PRL* **110**, 257201 (2013); Fishman, *PRB* **87**, 224419 (2013)]

This must be a combination magnon/phonon mode.

6. Numerical considerations

SW codes are trivially parallelized in wavevector **k**.

But for a spin state with M sublattices, we must diagonalize and obtain the eigenvectors for a 2M x 2M matrix with time cost ~M^2.

Consider some examples:

NiV_2O_4: **Q** = (0, 1, 0.4), M = 60
$CuFeO_2$: **Q** = (0.21, 0.21, 1.5), 2 layers, M = 200
$BiFeO_3$: **Q** = (0.5 + δ, 0.5 – δ, 0.5), δ = 1/222, 2 layers, M = 444
$MnWO_4$: **Q** = (0.22, 0.5, 0.52), 2 sublattices, M = 900

For $MnWO_4$, each **k** point requires about 4 minutes of CPU time.
To perform a thorough search over parameter space and to minimize over all the variational parameters is extremely time consuming.

7. Conclusions

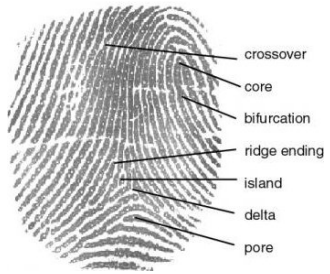

- The inelastic scattering spectrum provides a dynamical fingerprint of a complex spin state.

- To extract information from that fingerprint, we construct a variational spin state, minimize its energy, and compare the predicted and measured inelastic spectra.

- The FE state of the type II multiferroic $CuFeO_2$ is a distorted spiral with alternating small (~22°) and large (~132°) turn angles.

- The FE state of the type I multiferroic $BiFeO_3$ is a slightly distorted cycloid tilted out of the plane containing **Q** and **P**.

Collaborators

Theory:

Steven Hahn, Jun-Hee Lee, and **Satoshi Okamoto,** ORNL

Nobuo Furukawa, Aoyama Gakuin University, Japan

Jason Haraldsen, James Madison University

Shin Miyahara, Fukuoka University, Japan

Experiment:

Jaime Fernandez-Baca, Georg Ehlers, Masaaki Matsuda, Andrey Podlesnyak, and **Feng Ye,** ORNL

Tsuyoshi Kimura, Osaka University, Japan

Urmas Nagel and **Toomas Rõõm,** National Institute of Chemical Physics and Biophysics, Estonia

H. Engelkamp, High Field Magnet Laboratory, Nijmegen